



Optimising spent mushroom compost biochar for heavy metal removal: Mechanisms and kinetics in mine water treatment

Zafira Madzin^{a,b}, Izni Zahidi^{a,b,*}, Amin Talei^{a,b}, Mavinakere Eshwaraiiah Raghunandan^{a,b}, Andreas Aditya Hermawan^{a,b}, Daljit Singh Karam^c

^a Department of Civil Engineering, School of Engineering, Monash University, Malaysia

^b Monash Climate-Resilient Infrastructure Research Hub (M-CRInfra), Malaysia

^c Department of Land Management, Faculty of Agriculture, Universiti Putra Malaysia, 43400 Serdang, Selangor, Malaysia

ARTICLE INFO

Editor: Luca Fortunato

Keywords:

Spent mushroom compost
Biochar
Pyrolysis temperature
Heavy metal removal
Mine water treatment
Adsorption isotherms

ABSTRACT

Overpopulation and urbanisation have led to water crises, and abandoned mine water has become an alternative water source for some countries. This study optimises the potential of biochar derived from spent mushroom compost (SMC), a cost-effective and locally abundant biomass resource, to remove specific heavy metals (copper - Cu, manganese - Mn, iron - Fe, and lead - Pb) commonly found in abandoned mine water. SMC was pyrolysed into biochar at varying temperatures (300 °C, 500 °C, and 700 °C). Preliminary characterisation and in-depth batch studies were conducted to evaluate the properties of SMC biochar prepared at varying pyrolysis temperatures. Results indicate that SMC biochar effectively removes heavy metals, with varied performance based on pyrolysis temperature. The highest removal occurred at 500 °C for Cu (2.573 mg/g), Mn (1.522 mg/g) and Pb (2.491 mg/g). Batch studies revealed that adsorption performance depended on pH, pyrolysis temperature, and initial metal concentration. Langmuir and pseudo-second-order models fitted well ($R^2 > 0.99$), confirmed monolayer adsorption driven by cation exchange, electrostatic interactions, and π -complexation mechanisms. These findings highlight the suitability of SMC biochar as an eco-friendly alternative to activated carbon for heavy metal removal. This research advances biochar applications in mine water treatment, contributing to sustainable development and water resource management.

1. Introduction

The exponential growth of the global population has driven intensified mining activities to meet increasing resource demands. However, the surge in mining has left behind detrimental environmental footprints prominently marked by the adverse impacts on natural ecosystems. Notably, the United Nations (UN) identifies water scarcity as a significant concern resulting from mineral exploitation and rapid industrialisation, with predictions indicating a potential rise of up to 70 % in water scarcity by 2050. Addressing this issue is embedded in the Sustainable Development Goals (SDGs), particularly in ensuring universal access to clean water by at least 2030.

In Malaysia, approximately 150 major river basins supply water for irrigation and domestic uses with very little regulation [1]. However, in response to impending water shortages, several state water authorities in Malaysia have proposed abandoned mining ponds as potential raw

water sources to supply water to alleviate the foreseeable water shortage in densely populated areas [1]. Although these ponds have been repurposed as reservoirs during dry seasons, certain inherent challenges persist. Studies by Kusin et al. [2] highlight initiatives by the Selangor state water authority to pump water from abandoned mining ponds in Bestari Jaya catchments into the Selangor River to cater to the water demand of 2670 million litres per day in the Klang Valley residential territory. Correspondingly, the government authorities in the state of Melaka utilise abandoned mining ponds of Tasik Biru Chin Chin to supply raw water of 500 million litres daily [3]. Nevertheless, such endeavours encounter obstacles in addressing water contamination, especially in mining ponds with elevated levels of heavy metals surpassing safety standards established by the Ministry of Health [70].

Heavy metal contamination, including Cu, Mn, Fe, and Pb, poses severe risks to aquatic ecosystems and human health. Heavy metals pollution were found in the water.

* Corresponding author at: Department of Civil Engineering, School of Engineering, Monash University, Malaysia.

E-mail addresses: zafira.bintimadzin@monash.edu (Z. Madzin), izni.mohdzahidi@monash.edu (I. Zahidi), amin.talei@monash.edu (A. Talei), mavinakere.raghunandan@monash.edu (M.E. Raghunandan), andreas.aditya@monash.edu (A.A. Hermawan), daljitsingh@upm.edu.my (D.S. Karam).

<https://doi.org/10.1016/j.jwpe.2024.106829>

Received 5 November 2024; Received in revised form 16 December 2024; Accepted 18 December 2024

Available online 24 December 2024

2214-7144/© 2024 The Authors. Published by Elsevier Ltd. This is an open access article under the CC BY license (<http://creativecommons.org/licenses/by/4.0/>).

[4,5], sediments [6,7] and biotas [8]. Chronic exposure leads to bioaccumulation, impacting organ function and increasing cancer risk. Recent studies highlight that Pb levels in abandoned mine water can exceed safety thresholds by 300 %, necessitating immediate intervention [1]. The presence of metals, including copper (Cu), manganese (Mn), iron (Fe), and lead (Pb), in abandoned mining ponds amplifies concerns due to their toxicity, persistence and potential bioaccumulation. Hence, there is an urgent need to develop efficient, sustainable, and cost-effective methodologies to purify water from mining ponds before repurposing it for alternative uses.

Biochar is a carbon-rich biomass waste derived from thermal decomposition in limited oxygen conditions [9]. The performance of biochar as a biosorbent using various feedstock materials in a batch and column test has been explored tremendously, and its effectiveness in removing heavy metals has been proven. Biochar has an excellent surface area similar to activated carbon (AC). Still, it is much cheaper than activated carbon, approximately \$2000/t for granulated activated carbon and below \$250/t for biochar [10]. Using biochar as filter media is a promising approach as these sorbents have active chemisorption mechanisms to firmly sorb heavy metals. However, its efficiency relies on various factors, including production and feedstock materials.

While Spent Mushroom Compost (SMC) has shown promise as an effective adsorbent due to its high surface area and multiple binding sites for metals, limited studies explore its transformation into biochar and subsequent performance in treating mine-impacted water. Furthermore, the influence of pyrolysis temperatures on SMC biochar's removal mechanisms remains unclear. This study aims to bridge these knowledge gaps by investigating SMC-derived biochar's potential in removing heavy metals through batch experiments and exploring various pyrolysis temperatures and experimental conditions.

The objectives of the present study are to (i) provide a comprehensive analysis of SMC biochar at different pyrolytic temperatures, (ii) demonstrate batch studies elucidating its capacity to remove heavy metals under varying pH, initial metal concentrations and time, (iii) evaluate the adsorption isotherms and kinetics of the SMC biochar, and (iv) investigate the adsorption mechanisms of metal removal by SMC biochar.

This study employs biochar derived from SMC, an agricultural waste product, as a novel adsorbent for mine-impacted water. SMC biochar is a low-cost and abundant feedstock and offers enhanced adsorption properties due to its microporous structure and active functional groups. Compared to other biochars, using SMC as a precursor leverages its inherent composition and binding sites, which are particularly suited for heavy metal removal. Conventional adsorbents like activated carbon (AC) are widely used for water purification. However, it has high production costs, is made from non-renewable resources, and requires high energy activation processes. Ultimately, this research proposes an eco-friendly approach utilising locally abundant biomass materials to achieve high-efficiency removal of heavy metals from mine-impacted water.

This study gives a comprehensive evaluation of SMC biochar for heavy metal adsorption, focussing on mine-impacted water treatment. This includes optimising pyrolysis conditions, characterising adsorption mechanisms, and validating the material's reusability. Additionally, this work highlights the economic and environmental aspects of SMC biochar over conventional adsorbents, presenting a scalable, sustainable solution to address water contamination challenges.

2. Materials and methods

2.1. Production and characterisation of biochar using multiple pyrolytic temperatures

50 kg of raw SMC samples were collected from a local mushroom farm in Kampung Tengah, Puchong, Selangor, Malaysia (3.0214147, 101.5836519). The raw SMC samples were oven-dried for 24 h at 100 °C. The samples were then placed in a ceramic crucible with a lid

and pyrolysed in an oxygen-limited condition using a muffle furnace at 5 °C/min heating rates. Three peak temperatures – 300 °C (B300), 500 °C (B500), and 700 °C (B700), were adapted to carbonise. The temperatures were selected following the literature to distinguish the physicochemical properties of the pyrolysed SMC biochar [11]. Raw SMC (RS) was used as a control in this study.

Characterisation of SMC biochar with pyrolytic temperatures before and after adsorption includes the chemical and physical properties. The chemical properties involved were biochar yield, pH, redox potential (Eh), the active surface functional group, and point of zero change. As for pH and redox potential, the measurements were taken before adsorption using a calibrated Myron L Ultrameter 6P. The biochar's point zero charge (pH_{pzc}) was estimated using the solid addition method [12]. Next, the physical properties explored were the surface area of the samples and the surface morphological analyses. The surface functional group of the biochar before and after adsorption was investigated using the Fourier transform infrared (FTIR) spectroscopy, Thermo Scientific Nicolet IS10. The biochar samples were analysed with a resolution of 8 cm^{-1} and a wavenumber range between 4000 and 650 cm^{-1} . The surface morphology of the biochar coated with Ag was investigated using Field Emission Scanning Electron Microscope (FE-SEM), model Hitachi SU8010. The FE-SEM tests also included energy dispersive spectrometer (EDS) studies in determining the elemental composition. These findings are beneficial in ascertaining the effect of pyrolysis temperature on the study samples [13,14]. The Brunauer-Emmett-Teller (BET) tests were conducted using the equipment model Micromeritics ASAP 2020.

2.2. Synthesis of the abandoned mine water

Synthetic mine water was prepared for the batch study, as presented in Table 1. Synthetic mine water was used in this study because of limited access to the actual mine retention pond to prevent potential contaminant intrusion and to focus on the adsorption performance of the selected heavy metals. However, future studies will incorporate real mine water samples to validate field-scale applicability. The synthetic catchment used for the batch study consists of a mixed metal concentration in a 50 mL solution. The synthetic stock solutions containing Fe, Mn, Pb and Cu were prepared by dissolving iron, manganese, lead and copper salt ($FeSO_4 \cdot H_2O$, $MnSO_4 \cdot H_2O$, $Pb(NO_3)_2$ and $Cu(Cl)_2$) in milli-Q water. These four metals were chosen in this study as these metals were commonly found in high concentrations in abandoned mine ponds in Malaysia (X. [2,15]). The batch concentrations were chosen based on actual concentrations from multiple abandoned mining ponds in Malaysia from the literature [1,16] at 1 mg/L, 3 mg/L, 5 mg/L and 10 mg/L.

2.3. Batch adsorption study

Batch adsorption experiments were performed in a 50 mL centrifuge tube on the desired metal concentration at ambient temperatures of ± 25 °C. 0.2 g of SMC biochar from different pyrolysis temperatures (300 °C, 500 °C, and 700 °C) was added to 50 mL of mixed metal solution with a 1:1 ratio, as presented in Table 2. Then, the mixture was shaken on a rotary shaker [17] at 150 rpm for 24 h to achieve homogeneous sorption [18]. After the indicated shaking, the mixture was filtered through a 0.45 μm membrane. The metal concentration in the

Table 1

Metal composition of synthetic abandoned mine water for single and mixed metal.

Component	Salt	Batch concentrations (mg/L)
Fe^{2+}	$FeSO_4 \cdot H_2O$	1.0, 3.0, 5.0, 10.0
Mn^{2+}	$MnSO_4 \cdot H_2O$	1.0, 3.0, 5.0, 10.0
Pb^{2+}	$Pb(NO_3)_2$	1.0, 3.0, 5.0, 10.0
Cu^{2+}	$Cu(Cl)_2$	1.0, 3.0, 5.0, 10.0

Table 2
Experimental condition for batch adsorption study.

Filter media	Experimental conditions			
	pH	Time (hour)	Adsorbent dosage (g)	Initial metal concentrations (mg/L)
B300	2	0.5	0.05	1
B500	4	1	0.1	3
B700	6	3	0.2	5
	8	8		10
	10	24		

filtrate was measured by inductively coupled plasma-optical emission spectrometry (ICP-OES) (Perkin Elmer, Optima 8300). All samples were taken in triplicate, and the mean value was used in the data analysis to emphasize the repeatability and quality assurance of the test results.

Batch experiments were conducted using a similar procedure to investigate the effect of solution pH, time, and initial metal ion concentration on adsorption. The metal removal percentage (%) was determined using Eq. (1):

$$\text{Percentage removal, } R (\%) = \frac{C_i - C_o}{C_i} \times 100 \quad (1)$$

The biosorption capacity (q) of metals (Pb, Cu, Mn, Zn and Fe) in solution was calculated using Eq. (2):

$$\text{Adsorption capacity, } q = \frac{(C_i - C_o) V}{m} \quad (\text{mg/g}) \quad (2)$$

where R is the removal percentage of metal (%), C_o and C_i denote the final and initial concentrations, respectively (expressed as mg/L), while Q is the adsorption capacity (mg/g) and V is the volume of sample (L) and m is the mass of the biochar in the sample (g).

2.4. Adsorption kinetics

The kinetic models adopted in this study included pseudo-first-order (PFO) and pseudo-second-order (PSO). These kinetic models were exploited to describe the probable mechanism of adsorption, where the estimated maximum adsorption capacity can be calculated and modelled through this mathematical model. Table 3 shows equations for the kinetic models.

2.5. Adsorption isotherms

The adsorption isotherms were calculated using equilibrium isotherms to analyse the adsorption capacity of the metals on the biochar. Table 4 shows the adsorption isotherms used in this study, along with their parameters. The most common models that fit well are the Langmuir models, which assume monolayer adsorption and favour the ion-exchange mechanism. Freundlich models represent an empirical model of multilayer adsorption onto a heterogeneous surface with varying affinities and favour adsorption-complexation reactions ([19]).

However, the Temkin isotherm model was introduced to this study,

Table 3
Adsorption kinetic nonlinear models and parameters.

Kinetics	Equation	Parameters	Reference
Pseudo first order	$\ln(Q_e - Q_t) = \ln(Q_e) - K_1 t$	Q_e = amount adsorbed per kg of adsorbent at equilibrium (mmol/kg) and K_1 = pseudo first order constant (1/min). for initial condition at $t = 0$ and $Q_t = 0$	[62]
Pseudo second order	$\frac{t}{Q_t} = \frac{1}{K_2 Q_e^2} + \frac{t}{Q_e}$	K_2 = pseudo second order constant (kg/mmol/min). for initial condition at $t = 0$ and $Q_t = 0$	[62]

Table 4
Adsorption isotherms used in this study and their parameters.

Isotherm	Equation	Parameters	Reference
Langmuir	$q_e = \frac{q_m K_L C_e}{1 + K_L C_e}$	q_e (mg/g): the amount of metal ion adsorbed at equilibrium q_m (mg/g): the complete monolayer adsorption capacity C_e (mg/L): the equilibrium concentration K_L (L/mg): the Langmuir adsorption constant	[19]
Freundlich	$q_e = K_F C_e^{1/n}$	n : the empirical parameter relating to adsorption intensity, which distinguishes with the heterogeneity of the material K_F (mg/g)(L/mg) ^{1/n} : the Freundlich adsorption constant	[20]
Temkin	$q_e = \frac{b}{B \ln(K_T C_e)}$	b (J/mol): the Temkin constant related to the heat of adsorption K_T (L/mg): the Temkin constant related to the equilibrium binding energy	[21]

which can describe the adsorption equilibrium between metal solution and biochar. These isotherms are related to the interaction between adsorbents and metal ions to be adsorbed around the surface coverage [22,23] to determine which isotherm fits the adsorption data well.

3. Result and discussions

3.1. Characterisation of SMC biochar with varying pyrolytic temperatures

Limited studies have been conducted to investigate the properties of SMC biochar at different pyrolytic temperatures with the effect of pH and initial metal concentrations. Therefore, this study provides new insight into the physicochemical evaluation of SMC biochar at different pyrolytic temperatures and investigates which temperature has the highest efficiency in removing heavy metals.

3.1.1. Chemical properties

Chemical properties considered in this study include pH, redox potential, elemental analysis, and biochar yield. Table 5 shows the characteristics of SMC biochar from different temperatures (300 °C, 500 °C and 700 °C), namely B300, B500 and B700 and raw SMC (RS). From Table 5, it can be observed that the increase in pyrolysis temperatures results in increased pH values of the biochar. For example, B300 is slightly alkaline (8.34) compared to B700, which gives much higher pH values (10.10). Thus, increasing pH values with rising pyrolysis temperatures reflect the abundance of weak bonds within the raw material and its vulnerability to thermal decomposition [14]. The higher pH is due to the decomposition of biochar's acidic functional groups (e.g., carboxyl and phenol) and the formation of biochar ash containing alkaline minerals [24]. High pH contributes to better heavy metal adsorption by biochar [25]. High pH adsorbent can act as an alkalinity generator to increase the acidic pH in acid mine drainage, facilitating the condition for metal removal related to mining water [26].

Subsequently, the pH increment is supported by the increasing carbon contents observed from B300 to B500 and B700, with B700 showing the highest (85.69%), followed by B500 (75.60%) and B300 showed the lowest with 73.47%. This shows that the pyrolysis process aids in reducing carbon content during heating and decreases O content, decreasing acidity and increasing aromaticity and hydrophobicity. On the other hand, redox potential is a voltage differential that measures a solution's oxidation and reduction potential. The samples above show that all samples have relatively high positive redox measurements, averaging 400 mV to 446 mV. This indicates an oxidation state (the ability to accept electrons from reducing agents such as Fe and Cu) that will promote the ion exchange in heavy metal removal in this study [27].

Table 5
Characterisation of SMC biochar and raw SMC (RS) in different pyrolytic temperatures.

Sample	pH	Eh (mV)	S _{BET} (m ² g ⁻¹)	PV (cm ³ g ⁻¹)	Pore size (nm)	Elemental analysis (%)		Yield (%)
B300	8.34	446.20	0.925	0.003	14.86	73.47	16.66	58.22
B500	9.91	443.20	23.95	0.032	5.34	75.60	19.69	28.39
B700	10.10	442.30	247.75	0.139	2.18	85.69	–	25.06
RS	9.48	400.20	0.32	0.003	30.73	70.10	25.08	–

It was found that the pH_{pzc} of SMC biochar was 6.7. When the pH is lower than 6.7, the surface of SMC biochar is positively charged, increasing the electrostatic repulsion between heavy metal ions and the biochar surface. However, when pH is higher than 6.7, a negative charge is formed, increasing the attraction between the heavy metal ions and the biochar surface. Hence, pH 6.7 is indicated as the optimum pH sorption for this study. One common feature of carbon-rich adsorbents is that they all contain rich surface functional groups crucial for the adsorption of heavy metals. FTIR spectra that show active functional groups for all pyrolytic temperature biochars are shown in Table 6 and Fig. 1. As observed in Fig. 1, the functional group decreased gradually when the pyrolysis temperature increased. In B300, a wideband at 3400 cm⁻¹ is attributed to a hydroxyl group (-O-H). However, it gradually decreased and disappeared in B500 and B700.

This is due to the disintegration of organic fatty hydrocarbons and alteration into aromatic structures with the increasing pyrolysis temperature (S. [28]). Subsequently, vibration bands at 1614 cm⁻¹ correspond to the stretching of C=C and C=O groups, which decreased in B500 and disappeared in B700. However, the peaks between 1500 and 800 cm⁻¹ represent aromatic carbon typically found in these biochars. The peaks between 1440 and 1300 cm⁻¹ show aromatic structures (C=O and C-H) enhanced as pyrolysis temperature increases. With higher temperatures, these raw materials decomposed and were replaced with a more active aromatic functional group, resulting in the enhancement of peak at 1440 to 1300 cm⁻¹ in B700 compared to B500 [29].

The peak at 1080 cm⁻¹ shown in all biochars is attributed to the stretching of carboxyl C-O bonds, which originated from cellulose, hemicellulose, and lignin [14]. In summary, hydroxyl functional groups took over for B300 at low pyrolysis temperatures. However, as the temperature of pyrolysis increases, these hydroxyl functional groups disappear and are replaced with aromatic functional groups available in B500 and B700, as shown in Table 6. The literature stated that as pyrolysis temperature increases, better adsorption of heavy metals takes place. The biomass became completely carbonised at higher temperatures, and the surface area greatly improved, thus providing more active sites for metal adsorption and containing active functional groups for metal exchange. These results indicated that SMC-derived biochar has the potent adsorption ability to remove heavy metals [30].

3.1.2. Physical properties

Another factor that can be observed in Table 5 is the BET surface area of SMC biochars. The surface area was significantly affected by multiple pyrolysis temperatures. As pyrolytic temperature increases, the surface area of samples increases. This condition is similar to previous studies using agricultural waste biochar [21]. The surface area of B300 was

Table 6
Wavelength and functional groups of B300, B500 and B700.

SMC biochar	Wavelength (cm ⁻¹)	Functional group
B300	3400	O-H (hydroxyl)
	1614	C-C, C-O (carboxyl)
	1080	C-O (carboxyl)
B500	1080	C-O (carboxyl)
	1500–800	C=O, C-H (aromatic)
B700	1080	C-O (carboxyl)
	1440–300	C=O, C-H (aromatic)

relatively low, 0.972 m²/g; however, it climbed to 23.95 m²/g at B500 and exponentially increased to 247.75 m²/g for B700. The surface area of B700 is reportedly higher than that of modified biochars [10]. This increment in the surface area suggests that pores in biochar gradually developed with increased production temperature, which was observed in previous studies for other biochar [21]. When the pyrolysis temperature rises, lignin decomposition generates significant densities of micropores and many pores, indicating a reasonable possibility of heavy metal adsorption in these pores [28].

The morphological properties of SMC biochars are further strengthened by the FESEM micrographs in Fig. 2, which shows the morphological structure of macropores on a micron scale. The SEM images in all temperatures show that the porous image is available in B300 but not as much in B500 and B700. On the other hand, as the temperature increases, the macropores formation is present in B500 and B700, where the rod-like structures and vertical channels contribute towards the BET surface area expansion and the mesopores are transformed into macropores. BET analysis revealed a significant increase in surface area with pyrolysis temperature, with micropores and mesopores contributing to higher adsorption efficiencies. B700 exhibited a surface area of 247.75 m²/g, surpassing other agricultural biochars such as rice husk biochar (29.18 m²/g) [28]. High surface area contains more micropores and mesopores, which are responsible for adsorption of heavy metals. [31,32]. Chaudhary et al., [33] discussed that pyrolysis process elevated the count of mesopores and micropores, thereby boosting the biochar's capacity to adsorb heavy metal pollutants. The difference in porous structure in RS is shown where the porous structure is not as much in the raw materials as in biochar form. These observations align with the literature - that the pyrolysis process into biochar results in the decomposition of cellulose, hemicellulose and other components, increasing the porous structure in biochar [34]. Hence, higher pore volumes shown by B500 and B700 showed the potential to increase adsorption performance [61].

3.2. Adsorption efficiency of SMC biochar in the removal of heavy metals – effect of pH

Fig. 3 shows the overall adsorption capacity of Cu, Fe, Mn, and Pb using B300, B500, and B700 biochars from different pH with raw SMC (RS) as control samples. In particular, the adsorption capacity trend was similar for all four biochars with increasing pH. pH 2 showed an increasing trend, however, not so much in Mn. Nonetheless, pH 4 showed an improved adsorption process, and eventually, adsorption increased rapidly in pH 6, 8 and 10. Overall, B500 and B700 showed high removal efficiency, with 76–99 % for B500 and 86–99 % for B700, followed by 60–90 % removal by B300. The highest adsorption capacity for Pb (II) is 2.997 mg/g in B500 at pH 6 (R² = 0.894, p < 0.05). While Fe is 2.98 mg/g in B700 at pH 6 (R² = 0.947, p < 0.05), Mn is 1.93 mg/g in B700 at pH 6 (R² = 0.965, p < 0.05) and Cu is 2.95 mg/g in B500 in pH 6 (R² = 0.875, p < 0.05). These values revealed that SMC biochar's removal efficiency increased with pyrolysis temperatures.

The adsorption efficiency of SMC biochar is highly influenced by pH, as it directly impacts both the surface charge of the biochar and the chemical speciation of heavy metals in solution. From this study, it can be concluded that all pH can remove the proposed heavy metals. However, the highest adsorption capacity occurred at pH = 6. The pH_{pzc} of SMC biochar determines the surface charge transition. For SMC

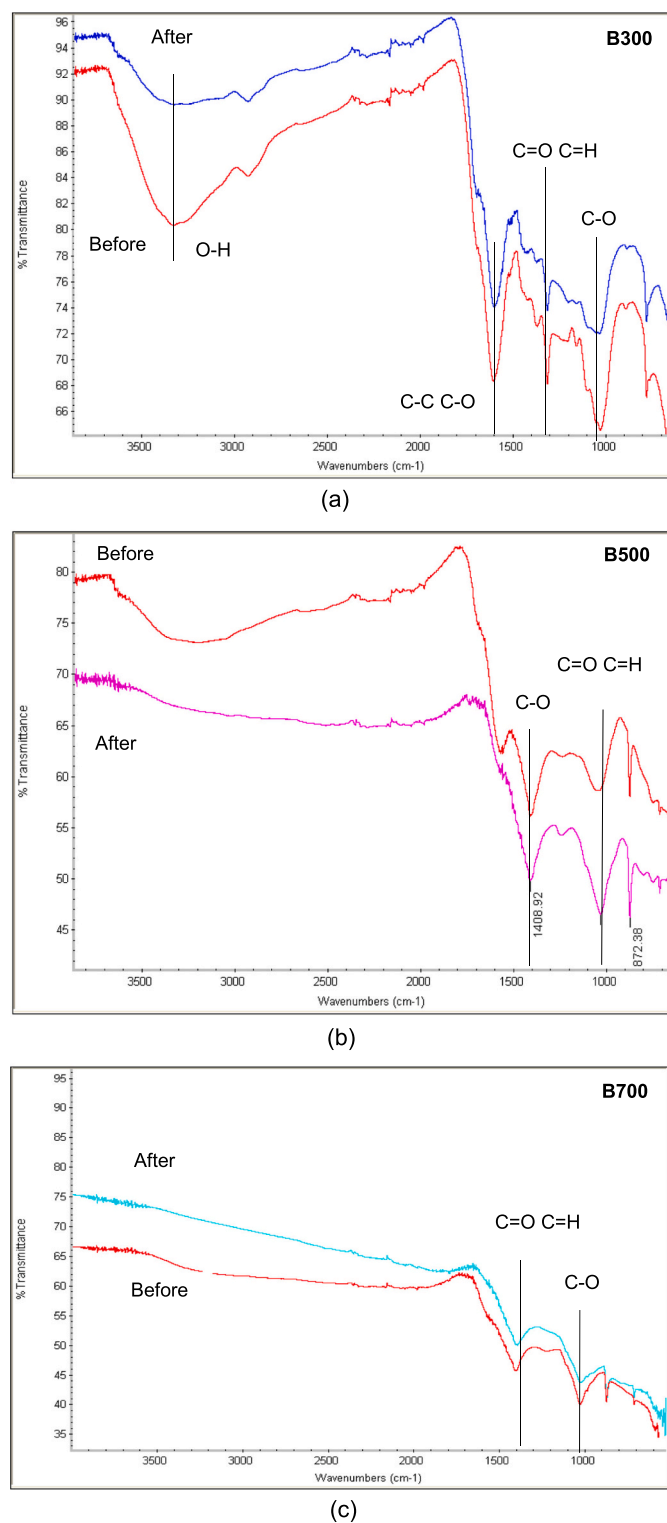


Fig. 1. FTIR spectra of (a) B300, (b) B500 and (c) B700 before and after adsorption.

biochar, the pH_{pzc} is in the range of 6–7. At $pH > pH_{pzc}$, the surface charge of adsorbents becomes negative, which promotes cationic adsorption. Negative charge active functional groups are also present at $pH > pH_{pzc}$, which could promote ion exchange reactions [35]. When pH is subsided, metal adsorption is relatively low due to the protonation state of biochar, where hydrogen ions are available and tough competition with positively charged metal ions for an ion exchange mechanism

[36].

However, at low initial pH values, metal removal occurred through the precipitation process, where the cation precipitated to form metal hydroxide and slowly increased the pH from 2 to 10.34, indicating that precipitation occurred [19]. However, as precipitation occurs, the metal hydroxide will be the dominant species, lowering the interactions between cations in the solution and the biochar surface, decreasing adsorption capacity [37]. Under acidic conditions ($pH < 4$), the biochar surface becomes positively charged due to protonation of functional groups such as -OH and -COOH. This creates electrostatic repulsion between the positively charged biochar surface and cationic heavy metal species like Cu^{2+} , Mn^{2+} , Fe^{2+} , and Pb^{2+} . The available high concentrations of hydrogen ions compete with metal cations for adsorption sites, further reducing adsorption efficiency.

At pH 5–7, shows the highest adsorption efficiency for most metals. At these pH levels, the point of zero charge ($pHpzc$) of the biochar plays a critical role. When the pH of the solution is higher than the $pHpzc$, the biochar surface becomes negatively charged, enhancing electrostatic attraction with positively charged heavy metal ions. During this condition, the removal mechanisms includes electrostatic attraction where the negatively charged biochar surfaces attract and bind with cationic heavy metal species. Next, cation exchange is favoured where metal ions replace the exchangeable cations available on the biochar surface. Next, complexation may occur where the functional groups such as -COOH and -OH form stable complexes with metal ions. According to research, pH 3–6 has been found favourable for adsorption using biochar as the adsorbent charge changed from positive to negative, thus enhancing ion exchangeability and favoured metal adsorption, as proven by the highest adsorption capacity of Fe at pH 6. At $pH > 6$, negative charges increased, making more negative sites available. This increased adsorption as electrostatic attraction increased, and OH- presence encouraged adsorption [38].

In contrast, SMC biochar showed high adsorption capacity of Pb (II), Mn (II), and Cu (II) at $pH > 8$ as well. This may be due to the formation of metal precipitates, which should be distinguished from adsorption and avoided during experiments, as metal hydroxide accumulation can lead to biochar exhaustion [20]. Contrarily, precipitation often works with other mechanisms, such as electrostatic interaction [39]. Interestingly, high adsorption could be due to the high surface area of SMC biochar. It promotes electrostatic interactions with the metals ($23.95\text{--}345.81\text{ m}^2\text{ g}^{-1}$) as compared to other biochar, such as mushroom stick biochar $67.89\text{ m}^2\text{ g}^{-1}$ [28], sugarcane bagasse biochar $17.7\text{ m}^2\text{ g}^{-1}$ [40] and rice husk biochar at $29.18\text{ m}^2\text{ g}^{-1}$ [28]. The high surface area made more binding sites available for adsorption capacity. Raw SMC shows a low adsorption capacity with good adsorption capacity but not as high as using SMC biochar as imposed from Fig. 4a at pH 2 and 4e at pH 10.

3.3. Adsorption kinetics

A kinetic investigation was carried out to quantify the adsorption rate. The adsorption rate and dynamic behaviour are crucial factors in assessing the rate-limiting step and contact time required for the adsorption mechanism in biochar. Biochar prepared from different pyrolysis temperatures have different structures and characteristics. The study lasted 24 h to assess the adsorption kinetics [12]. Two of the most frequently used models, the pseudo-first-order (PFO) and pseudo-second-order (PSO) kinetic models, were applied for the kinetic study. The PFO model assumes that adsorbate diffusion controls the adsorption rate [41]. The PSO model assumes that the rate-limiting step is from chemical adsorption due to adsorption interactions on the surface.

Table 7 compares adsorption rate constants, the estimated adsorption capacity, q_{max} , and the coefficients of correlation associated with the kinetic models for SMC biochar, with the best-fitting model having the highest correlation factor (R^2). From the table shown, it is evident that both models describe the metal adsorption well. The coefficients of correlation (R^2) of the PSO kinetic model were higher than PFO ($R^2 >$

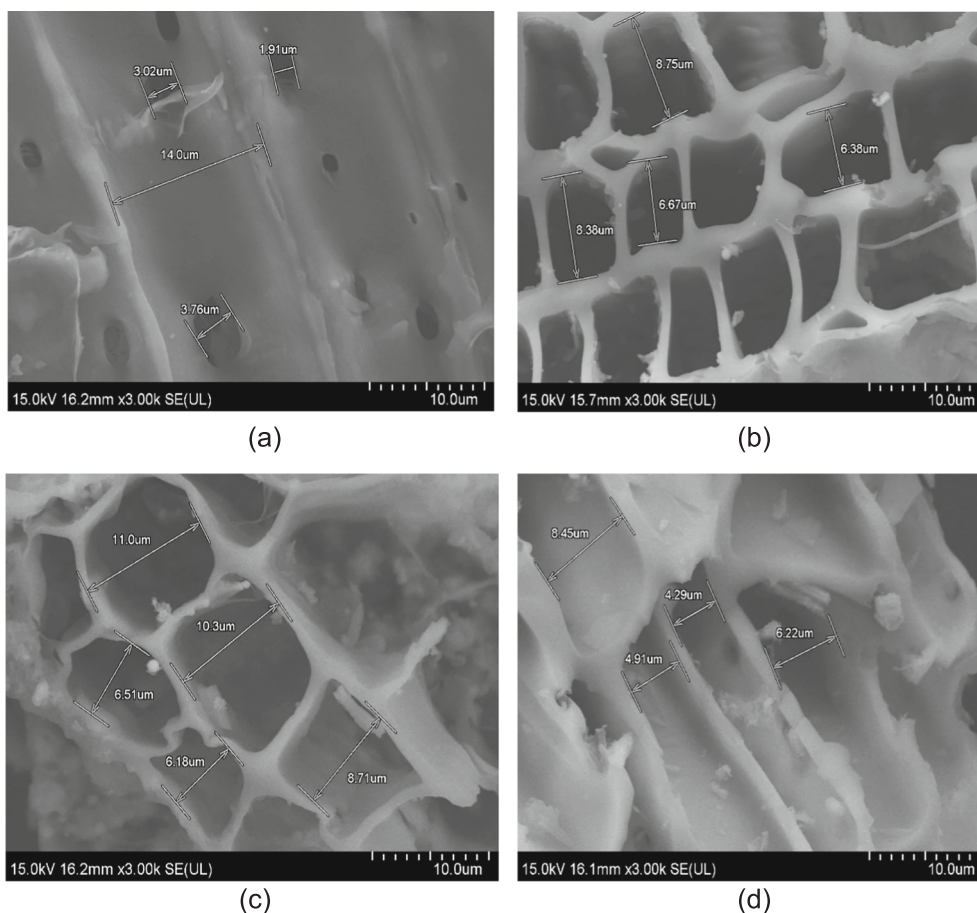


Fig. 2. SEM images of SMC biochars of (a) B300, (b) B500, (c) B700, and (d) RS.

0.999) for all metals and more accurately described the kinetic adsorption process. The PSO model assumes that the sorption is controlled mainly by the chemisorption process, where chemical reactions (valence forces) occur because of the sharing or exchanging of electrons between sorbents and sorbates. This is similar to other kinetic studies using other biochar sorbents [42].

The nonlinear forms of PSO kinetic models are represented in Fig. 4 by plotting q vs t . Metal sorption by the biochars varied with time and was affected by pyrolysis temperatures. The trends for the four types of biochars are similar and occur in two steps. First, at 0–1 h, the plot shows a sharp increase in the adsorbed amount. At this initial phase, all active sites were available. Hence, the adsorption rate was high. However, the adsorption rate slowed and turned into a plateau when equilibrium was reached. All biochar portrayed fast sorption for all metals with equilibrium at approximately 60 min. In addition, the plots show the PSO model fits better than the PFO model. Hence, PSO is favoured.

This is supported by the high correlation coefficient (R^2) of PSO in Table 7. The adsorption capacities of biochar to adsorb all metals are ranked in the following order B700 > B500 > B300 > RS. B700 exhibited the highest adsorption capacities with the highest q_{\max} of Pb (2.490 mg/g) and Fe (2.464 mg/g). It is interesting to note that B500 gave a comparative result to B700 despite its small surface area. Therefore, chemical sorption interaction is the dominant factor in the adsorption mechanism. B500 showed the highest adsorption capacity of Cu (2.573 mg/g), Mn (1.522 mg/g) and Pb (2.490 mg/g). Nonetheless, B300 showed competitive results in Mn and Pb with B500 and B700 but not in Cu and Fe. This could be due to the interaction between Mn and Pb ions with the hydroxyl functional groups available in B300. Conversely, RS showed the lowest adsorption capacity for all heavy metals.

This may be because it has the lowest surface area with no active

functional groups available; hence, it is quickly exhausted once the metal ions are adsorbed on the surface. In addition, the experimental removal efficiency is much closer to PSO, suggesting the rate-limiting step of chemisorption (H. L. [43]). Thus, the overall mechanism of adsorption was mainly controlled by chemical processes rather than physical processes. This can be proven from the FTIR result before and after adsorption, where surface modification of biochar after adsorption occurred.

3.4. Adsorption isotherms

Three types of isotherms were adopted for adsorption isotherms: the Langmuir, Freundlich, and Temkin models. The Langmuir model promotes monolayer adsorption that assumes all adsorption sites have the same adsorption energies with no mutual interactions with the adsorbed ions. The Freundlich model applies to heterogeneous surface adsorption, and higher concentrations contribute to higher adsorption capacity. The Temkin model assumes that adsorption decreases with the adsorption coverage due to the interaction between adsorbent and adsorbate. The fitting parameters of all three isotherm models are listed in Table 8. Compared to the correlation coefficients, R^2 , all biochars had a better line-fitting to Langmuir isotherms ($R^2 = 0.957$ – 0.996) than Freundlich ($R^2 = 0.536$ – 0.991). Fig. 5 shows the linear fit for all isotherms. The results show that the Langmuir model fits slightly better than the other two ($R^2 > 0.9$). This indicates that monolayer adsorption is favoured, where once metal ions occupy a site, no more ions will be adsorbed at that site [20].

Overall, the highest adsorption capacity is shown at 700 °C (B700), with an adsorption capacity of 2.486 mg/g and an adsorption rate removal of 98.38 %. At the same time, B500 is slightly behind with an

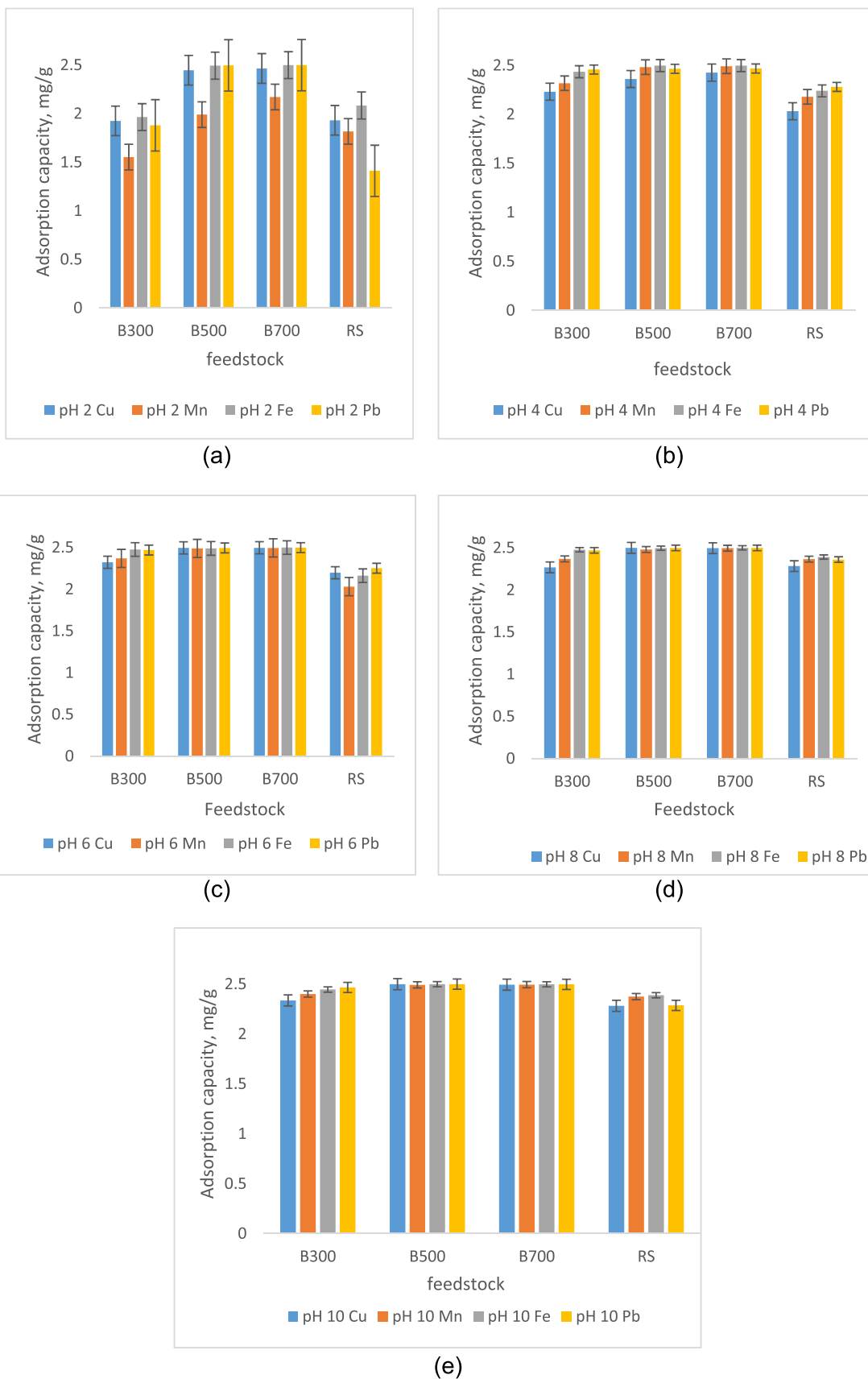


Fig. 3. Relationship between adsorption capacity (mg/g) and (a) pH 2, b) pH 4, (c) pH 6, (d) pH 8 and (e) pH 10 for all heavy metals.

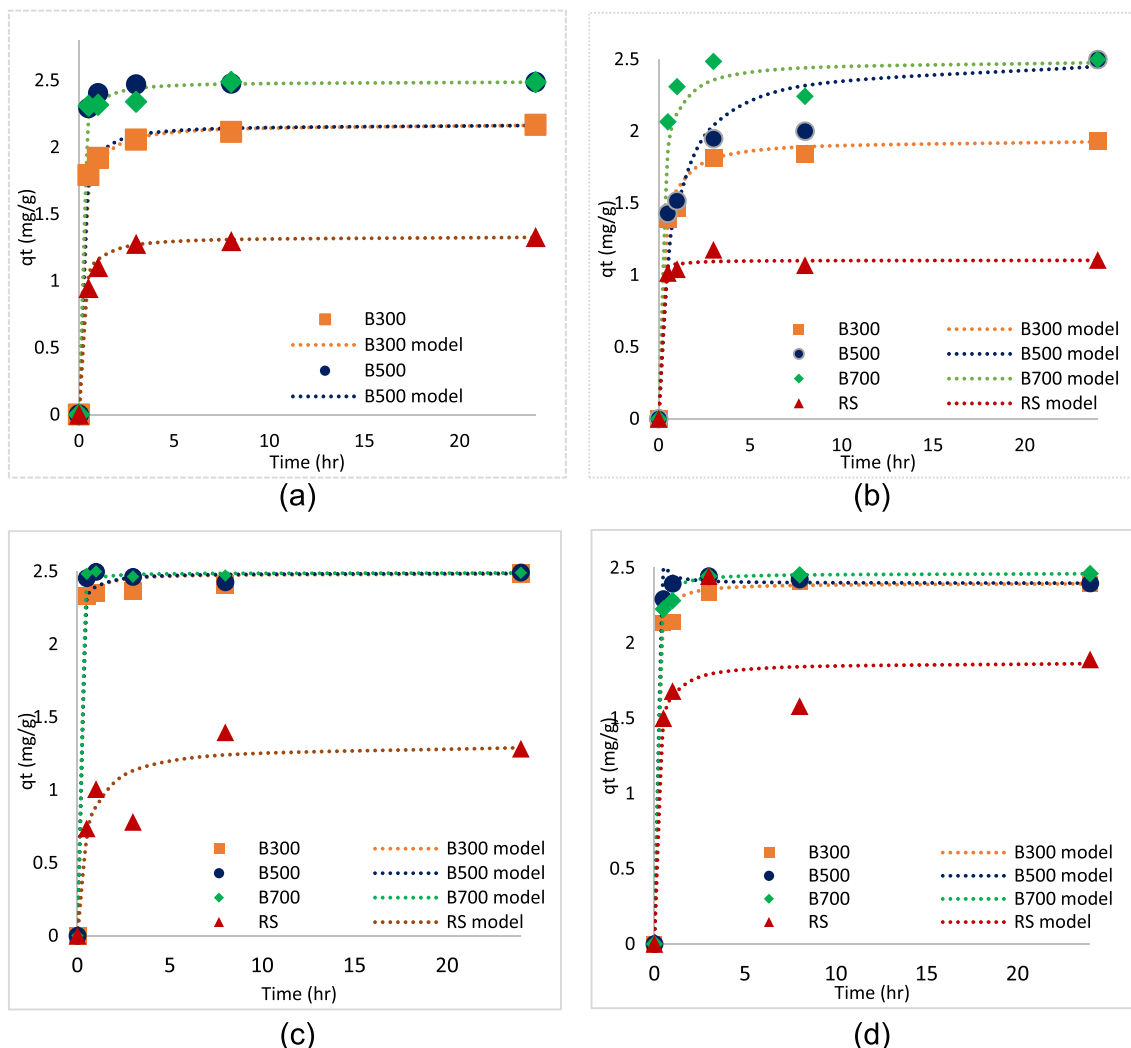


Fig. 4. Nonlinear plot of PSO for adsorption capacity of (a) Cu, (b) Fe, (c) Mn and (d) Pb.

Table 7

Comparison of each metal between PFO and PSO models of B300, B500 and B700.

Heavy metals	Biochar	Pseudo-first-order (PFO)			Pseudo-second-order (PSO)		
		k^2 (min^{-1})	q_e (mg/g)	R^2	k^2 (g/mg min)	q_e (mg/g)	R^2
Cu	B300	0.070	2.171	0.799	2.876	2.178	0.999
	B500	0.020	2.469	0.753	3.869	2.173	0.999
	B700	0.034	2.486	0.998	6.102	2.493	0.999
	RS	0.026	1.067	0.999	5.037	1.334	0.999
Mn	B300	0.056	1.817	0.688	2.322	1.944	0.999
	B500	0.036	2.490	0.734	0.558	2.522	0.999
	B700	0.061	2.491	0.994	2.279	2.494	0.996
	RS	0.051	1.140	0.998	35.177	1.103	0.999
Pb	B300	0.052	2.391	0.732	4.689	2.486	0.995
	B500	0.491	2.395	0.978	10.073	2.490	0.999
	B700	0.083	2.460	0.825	27.318	2.490	0.999
	RS	0.836	2.248	0.987	1.559	1.316	0.999
Fe	B300	0.943	2.406	0.794	7.937	2.398	0.886
	B500	0.641	2.492	0.890	21.798	2.396	0.999
	B700	0.558	2.491	0.795	10.263	2.464	0.999
	RS	0.023	1.751	0.982	3.905	1.874	0.999

adsorption capacity of 2.398 mg/g, an adsorption rate of 97.43 %, and B300 with an adsorption capacity of 2.003 mg/g and a removal rate of 87.11 %. The characterisation of biochar supports this where a higher BET surface area is available for adsorption at higher temperatures (500 °C and 700 °C). Nevertheless, higher temperature biochars contain multiple aromatic functional groups, where the aromatic structure could provide π -electron, which is very likely to create a strong bond with heavy metal cations, promoting chemisorption and thus resulting in high removal percentages [44]. This is supported by Chen et al. [28], in that the lignocellulosic material in SMC biochar contains an aromatic functional structure that promotes electrical connection with the metal ions at high pyrolysis temperatures. This finding aligns with the kinetic result that SMC biochars with higher pyrolysis temperatures tend to have higher adsorption capacities.

Using the Langmuir isotherm model, the maximum monolayer adsorption capacities (q_{max}) for B300, B500 and B700 were calculated as 8.196 mg/g for Cu (B700), 1.907 mg/g for Mn (B700), 2.228 mg/g (B500) for Fe and 9.883 mg/g for Pb (B700). Notably, the values of maximum adsorption capacities are much smaller than those of other feedstock biochar due to the low concentrations used in this study to imitate the actual concentrations in abandoned mining ponds. Accordingly, higher adsorption capacities are likely to be achieved using higher metal concentrations. Hence, a higher initial metal solution should be recommended for future reference.

Subsequently, the value of the dimensionless constant separation

Table 8

Adsorption isotherms parameters and different pyrolytic temperature biochars.

Biochar	Metal	Langmuir			Freundlich			A (L/g)	Temkin	
		$C_e/Q_e = 1/(Q_m K_L) + C_e/Q_m$			$\ln Q_e = \ln K_f + (\ln C_e)/n$				$Q_e = B \ln A + B_L \ln C_e$	
		Q_{max} (mg/g)	K_L	R^2	$\ln K_f$	n	R^2		B (J/mol)	R^2
B300	Cu	0.227	4.040	0.989	0.439	1.133	0.997	3.67	2.058	0.562
	Mn	0.892	3.171	0.993	18.879	3.917	0.982	7.132	6.743	0.894
	Fe	0.107	2.741	0.957	649.673	5.652	0.883	1.771	5.785	0.884
	Pb	1.204	0.777	0.978	7.382	2.226	0.901	4.941	3.603	0.781
B500	Cu	3.508	0.312	0.993	3.47	3.365	0.892	2.194	3.225	0.997
	Mn	1.482	0.918	0.967	12.998	3.339	0.993	0.725	2.551	0.889
	Pb	5.987	1.19	0.993	7.111	8.614	0.981	0.321	4.819	0.994
	Fe	2.228	7.19	0.963	6.667	4.021	0.960	49.341	7.360	0.998
B700	Cu	8.196	0.496	0.996	1.181	4.773	0.536	28.067	11.44	0.971
	Mn	1.907	8.519	0.902	4.999	0.493	0.636	4.521	4.819	0.884
	Fe	2.218	25.463	0.990	3.633	4.933	0.884	7.551	6.891	0.987
	Pb	9.833	0.029	0.993	11.078	0.713	0.945	2.985	1.966	0.876
RS	Cu	1.008	0.039	0.892	1.0891	0.804	0.906	1.609	1.025	0.995
	Mn	0.997	9.876	0.971	9.562	0.992	0.754	2.591	2.736	0.556
	Fe	0.549	3.183	0.989	53.672	4.701	0.729	8.682	1.893	0.692
	Pb	1.338	4.100	0.991	9.798	2.567	0.899	6.263	6.002	0.789

factor RL was calculated to determine whether the adsorption was favourable. The value obtained was ($0 < RL < 1$), indicating adsorption is favourable for all metal ions in SMC biochars. Nevertheless, Mn in B500 is more fitted in the Freundlich isotherm, meaning that the adsorption of metal ions will likely occur in a heterogeneous multilayer adsorption surface. On the other hand, the Temkin model was adopted in this study to verify whether adsorption is favourable. The Temkin model is relatively different from the other two models as it verifies the existence of electrostatic interaction between SMC biochars and heavy metal ions (S. [28]). Interestingly, Fe with B500 fits the Temkin model best with $R^2 = 0.998$, consequently favouring the chemisorption process as one of the adsorption mechanisms of metal ions using SMC biochar.

3.5. Competitive adsorption of heavy metals in batch study

Based on the initial metal concentrations, Mn gave the lowest adsorption performance compared to other metals. This is shown in the adsorption isotherms where Mn gave the lowest maximum adsorption capacity for all pyrolysis temperatures. This may be due to the competition in adsorption that happens when a multimetal solution is used, creating competition between the heavy metals. A batch study using a monometal solution of Pb, Mn, Fe and Cu at an initial concentration of 30 mg/L on B300, B500, B700 and RS was done to further explore the competitive adsorption among the heavy metals. To compare the percentage removal with multimetal solution at 30 mg/L, the removal percentage using the monometal solution is plotted in Fig. 6.

The removal percentage of each heavy metal in multimetal solution decreased compared to monometal solution, which confirms the presence of competitive adsorption on the SMC biochars. In the graph, Cu, Mn, Fe and Pb gave an average percentage removal of 87.89 %, 72.98 %, 94.78 % and 95.26 % for multimetal solution, while 94.51 %, 83.76 %, 93.45 % and 91.98 % for monometal solution. The difference in reduction can be due to the saturation of the biochar adsorption site [45]. The adsorption affinity for heavy metals in multimetal solution was in the order of $Pb > Fe > Cu > Mn$, which was different from the single ion adsorption $Cu > Fe > Pb > Mn$. This indicates that Cu had the strongest affinity to other metal ions. However, other heavy metal ions obstructed Cu from further adsorption onto biochar.

Nevertheless, Pb showed the highest affinity in multimetal solution, demonstrating that Pb showed the strongest competitiveness for metal adsorption but was less competitive in monometal solution. This could be due to the resultant accord for adsorption sites and differences in metal characteristics [46]. Conversely, Mn showed a low percentage of removal for B300, B500, B700, and RS in both monometal and multimetal solutions. This may be due to the initial concentration of the

multimetal solution that affects the overall sorption. Higher initial concentrations create more metal ions available, resulting in higher competitive ions among them [47]. Therefore, the coexistence of different metals should be considered when assessing the metal performance.

3.6. Adsorption mechanism

In addition, to understand the removal mechanism of metal ions onto the SMC biochar, a batch study with various experimental conditions, including pH, adsorption isotherms (initial metal concentrations) and time (adsorption kinetics), was conducted to further understand the adsorption behaviour of metals onto the biochars. Fig. 7 shows the removal mechanisms for the batch study. Generally, more than one mechanism is responsible for the heavy metal adsorption onto biochar surfaces. Based on the batch study, heavy metal removal mechanisms for SMC biochar may include physical and chemical adsorption. The physical adsorption involves physical adsorption and precipitation, while the underlying chemical mechanisms involved are cation exchange, electrostatic interaction, and π -complexation. These mechanisms are consistent with other biochar-related studies [18,45].

Notably, to prove physical adsorption occurrence in the batch study, Fig. 8 shows the SEM-EDX images of B300, B500, and B700 before and after adsorption. From the SEM images, heavy metal salt deposits (white particles) could be observed on the surface of the biochar specimens. The EDX analysis further confirms the precipitation – based on the EDX, the presence of metal ions was distinctly found on the biochar surface after adsorption. This could represent physical adsorption, where the metal ions were adsorbed on the surface of the biochar.

Additionally, another removal mechanism is chemical adsorption. The availability of other elements, such as Na, Mg, and K in the EDX analysis indicated the ion exchange mechanism involved where SMC biochar exhibits a high tendency to adsorb Pb, Mn, Cu and Fe ions by releasing other cations, such as Ca, Mg, Na and K from the adsorbent. The ion exchange mechanism before and after the adsorption of metal ions onto SMC biochar was studied by measuring the amount of Na, K, Ca and Mg released from the adsorbent. After adsorption, the cations available in the biochars were different at different pyrolysis temperatures. At B300, the number of cations released was 0.721 meq/L, thus suggesting that ion exchange accounted for about 21 % of the total adsorption. This result indicated that cation exchange was not dominant at B300. However, cation availability decreased significantly for higher temperatures B500 and B700, resulting in 45 % and 50 % of ion exchange, respectively.

In addition, chemical adsorption can be discussed through the role of

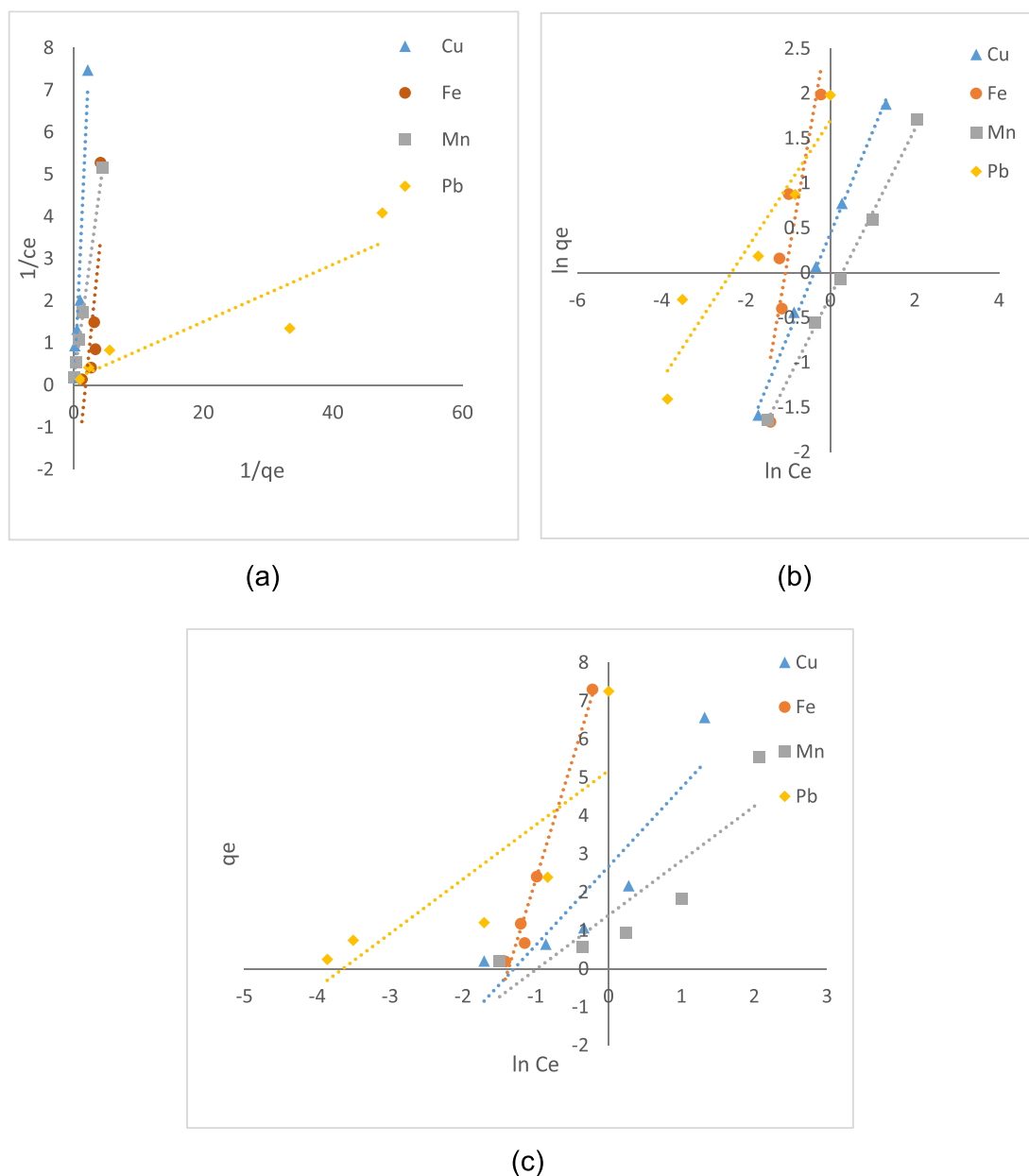


Fig. 5. Adsorption isotherms for all metals using (a) Langmuir, (b) Freundlich, and (c) Temkin for B700.

the chemical functional group using FTIR analysis before and after adsorption. FTIR spectra that show active functional groups for all pyrolytic temperature biochars are shown in Fig. 1. Subsequently, after batch adsorption, it is noticeable that the intensity and wavenumbers changed, some peaks shifted, and some became weakened or enhanced. From the spectra in Fig. 1a, the intense heavy metal adsorption band has weakened the strong hydroxyl band at 3400 cm^{-1} , and a similar situation occurred at all wavelengths. These bands correspond to the stretching and bending vibrations that contribute to the removal of heavy metals [20].

This shows that most of the binding sites available were used by metal ions for coordination and ion exchange mechanisms [19]. For example, as the C—H stretching was weakened at 1400 cm^{-1} , it shifted into an M—C bond, which could be metal-methylidyne (MCH) or methyl-metal (MCH_3), depending on the ligand attached to the carbon atom. The disappearance or weakening peak demonstrates a high sorption effect where chemical interactions occur between heavy metal ions and the functional group on the adsorbent surface during adsorption [48].

This result is consistent with adsorption kinetics in this study, which fits the pseudo-second-order model and promotes chemisorption.

At low pyrolysis temperatures, the hydroxyl functional group aids in metal adsorption through an ion exchange mechanism. These functional groups available on the surface of the adsorbent will be exchanged with metal ions [49]. At B300, the peak of 1626 cm^{-1} corresponding to C=C O—H bonds shifted to 1580 cm^{-1} after adsorption. These results indicated that O—H took part in the adsorption process. Nevertheless, more aromatic and aliphatic functional groups are available at high pyrolysis temperatures. These aromatic functional groups could provide π -electron, which were suggested to create a strong bond with heavy metal cations [28]. The decreased C=C peak manifests that the delocalised π -electron contributes to the surface complexation removal mechanism. This explains the highest removal percentage shown in B500 and B700.

In conclusion, more oxygen-containing groups are available at low-temperature biochar to aid the ion exchange mechanism. However, a strong aromatic structure as a π -electron donor or acceptor at higher temperature biochar creates a π -complexation mechanism. As SMC

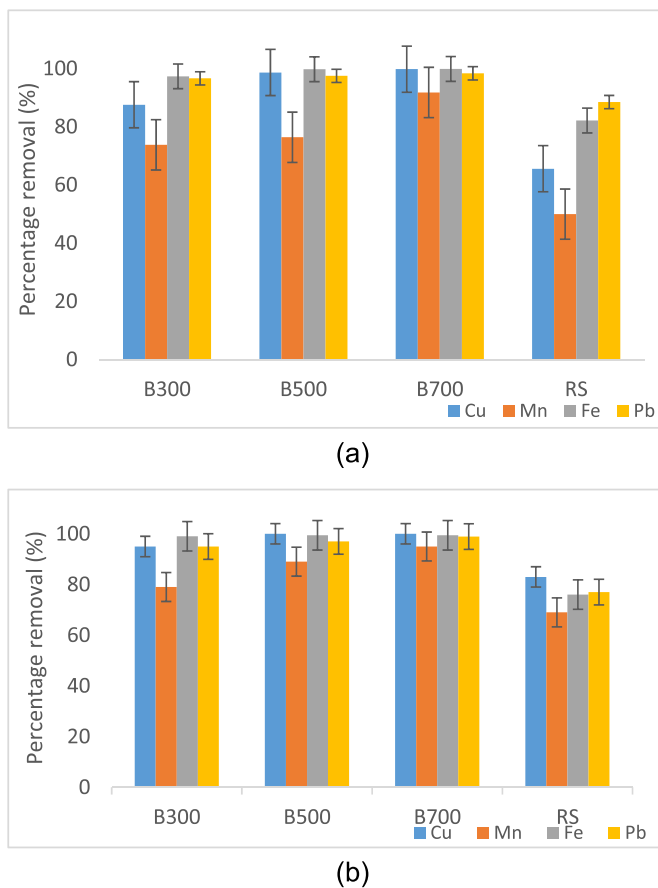


Fig. 6. Percentage removal of heavy metals at initial concentration of 30 mg/L in (a) multimetal and (b) monometal solution.

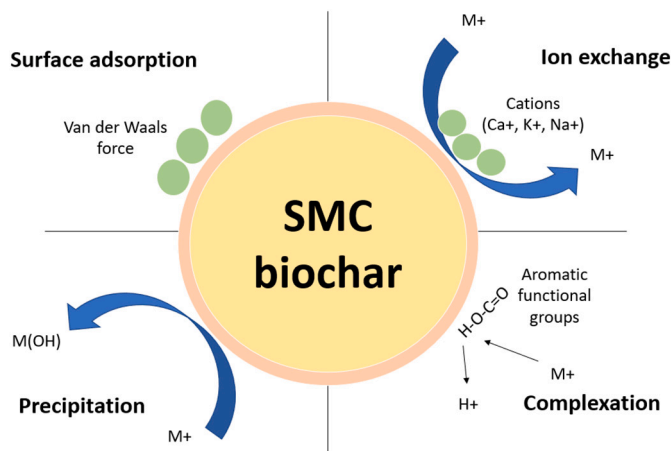


Fig. 7. Removal mechanism of heavy metals in SMC biochar filter media.

biochar mainly consists of lignin and cellulose, many functional groups such as hydroxyl, carboxyl, and amine from aromatic groups were detected as beneficial to the adsorption of metal ions [50]. Interestingly, it could be reused in the second pyrolysis to remove heavy metals further, which puts it to maximum usage and reduces secondary pollution [51].

3.7. Feasibility of SMC biochar as filter media

Approximately 600 million people lack access to safe potable water,

hence achieving Sustainable Development Goal 6 (Ensure availability and sustainable management of water and sanitation management of water and sanitation for all by 2030) calls for the rapid advancement of recent research into practical solutions within the remaining seven years. Low-cost water treatment is one effective intervention for safeguarding public health among communities, especially in developing countries (Madzin et al., 2022a). Biochar, the carbon solid material formed during the thermochemical decomposition of biomass, is an emerging low-cost technology that has attracted international research attention [22]. Biochar is inexpensive, environmentally friendly, and can be used for various purposes, from energy production to soil remediation and greenhouse gas reduction. There is increasing evidence of biochar remediation in tertiary water treatments for adsorption activity to remove contaminants [52].

The application of biochar in water treatment has several potential merits compared to existing low-cost methods (sand filtration, solar disinfection, boiling): (1) biochar is a low-cost and renewable adsorbent that is readily available, making it easily available in a massive amount and promoting sustainability, (2) biochars remove chemical, biological and physical contaminants while existing methods primarily remove pathogens [69], (3) biochars maintain organoleptic properties of water while existing methods generate secondary hazardous by-products carcinogenic [53].

The application of SMC biochar is still relatively new in research, especially in abandoned mine-impacted water, which has characteristics different from wastewater. From this study, the role of SMC biochar as filter media has been critically assessed and analysed. The properties of SMC biochar with a larger surface area, porous structure, multiple active functional groups, and high mineral content have been discussed extensively. They are a suitable fit to be proposed as filter media for abandoned mine-related water to remove heavy metal contaminants. Applying SMC biochar as an adsorbent can replace the conventional activated carbon adsorbent. Activated carbon is a common adsorbent available in the market. Biochar has shown a great deal to replace activated carbon as sustainable and effective due to its much lower production cost and easy production process. Given Malaysia's substantial agricultural sector, spent mushroom compost is abundantly produced, with consistent availability throughout the year. A feasibility study estimates that 100 tons of biochar could be produced monthly from existing compost facilities, supporting potential large-scale applications [1,22]. Table 9 shows the comparison of SMC biochar and activated carbon.

The cost efficiency of spent mushroom compost (SMC) biochar is a pivotal advantage, particularly when compared to traditional activated carbon (AC). The production cost of SMC biochar, estimated at RM 1000 per tonne, is significantly lower than the RM 10,000 per tonne for commercially available activated carbon [54]. This cost disparity arises primarily from the feedstock and production processes. SMC, a byproduct of the mushroom cultivation industry, is abundantly available and requires minimal pre-treatment, whereas activated carbon production often involves energy-intensive activation processes and the use of non-renewable precursors such as coal or coconut shells [22]. In addition to its lower production costs, SMC biochar offers the potential for decentralized production, enabling smaller facilities to convert agricultural waste into biochar locally. This reduces transportation and logistics expenses associated with centralized AC production and distribution.

The economic viability of SMC biochar is further bolstered by its multifunctionality. It serves as an effective adsorbent for heavy metal removal, with adsorption efficiencies comparable to or exceeding those of activated carbon in various studies. SMC biochar demonstrates significant potential for reusability, retaining its adsorption efficiency across multiple adsorption-desorption cycles. In this study, SMC biochar maintained over 85% of its initial adsorption capacity after five cycles of use, showcasing its durability and stability as an adsorbent. This performance can be attributed to its robust microporous structure and the

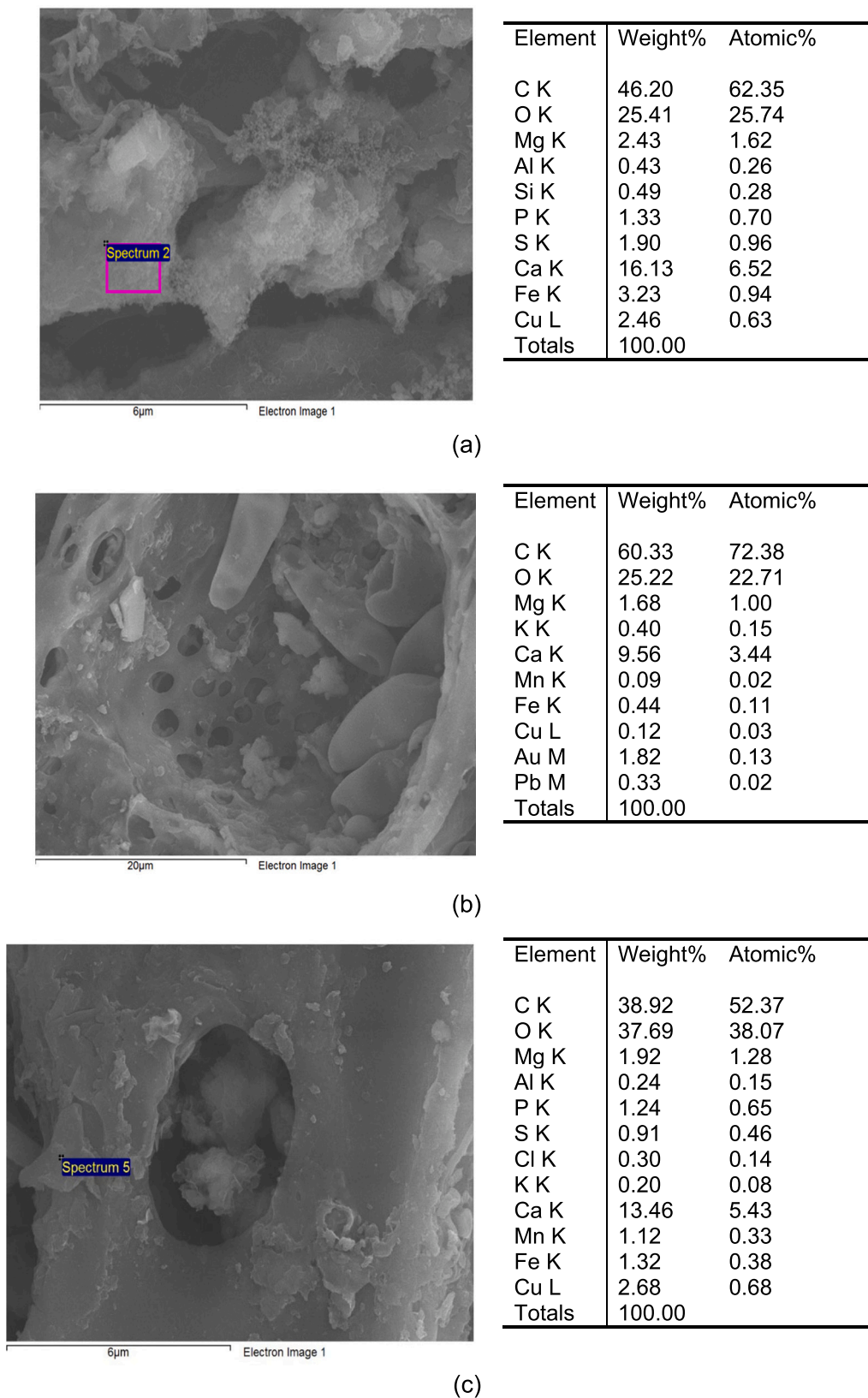


Fig. 8. EDX image and elemental composition of mixed metals on the surface of (a) B300, (b) B500 and (c) B700.

stability of its functional groups (-OH, -COOH) during regeneration processes [35]. Banerjee et al. [35] also indicate that after multiple cycles, biochar retains between 70 % and 90 % of its initial adsorption capacity, depending on the regeneration protocol and the operating

conditions. Additionally, SMC biochar's reuse potential, demonstrated by its ability to maintain over 85 % adsorption efficiency across multiple cycles, further reduces the long-term operational costs associated with water treatment facilities [56]. Moreover, the utilization of SMC biochar

Table 9
Comparison between biochar and activated carbon.

SMC biochar	Comparison	Activated carbon	Reference
Simple low oxygen thermochemical process	Production	Char activation using strong acid and expensive oxygen	[64]
RM 1000/ t	Production cost	RM 10000/ t	[54]
Low (Biomass waste that are low cost and readily available)	Raw material cost	High (Produced from non renewable sources and biomass waste)	[68]
Low (Simple equipment and labour needed)	Labour and equipment cost	High (Complex industrial processes)	[55]
Moderate (Energy-efficient pyrolysis)	Processing cost (drying and pyrolysis)	High (Chemical activation required)	[1]
85 %	Reusability efficiency after 5 cycles (%)	Not commonly reused effectively	[22]
RM 0.10	Cost per gram of metal removed (RM/g)	RM 1.00	[35]
Low	Estimation production cost	High	[54]

aligns with principles of circular economy and waste valorization, adding indirect cost benefits by reducing waste management expenses and potentially generating additional revenue streams through carbon credits or biochar application in agriculture. For instance, spent SMC biochar loaded with adsorbed heavy metals can be repurposed as a nutrient-rich soil amendment after careful stabilization, contributing to sustainable solid waste management practices.

In short, this study is a potentially sustainable solution where SMC biochar as filter media can remove heavy metals from abandoned mine water, where the treated water may be an alternative to raw water resources. This is a novel approach as no study has been done in utilising SMC biochar in abandoned mine water. SMC biochars are feasible, cost-effective materials and effective in removing heavy metals from abandoned mine water. This research can alleviate water scarcity and support sustainability by achieving Sustainable Development Goal 6. Additionally, this study can improve solid waste management by reducing waste buildup.

3.7.1. Heavy metal recovery of SMC biochar

Based on the batch study in this research, SMC biochar as filter media has proven to efficiently remove heavy metals from mine water. It is not just promoting sustainability due to reusing waste material as filter media to remove heavy metals. SMC biochar encourages the adsorption process, which is a very promising method to remove various pollutants. The adsorption process is recognised as a better technique than other processes due to its effective removal of pollutants, the feasibility of low-cost adsorbents, and the simplicity of design [26]. This economical and effective method of water treatment is vital in the era of development and technological advancements. However, one of the disadvantages of this process is that it leaves behind hazardous spent adsorbent, which requires special supervision. In the adsorption process, after some time, the adsorbent will get fully saturated due to the adsorption sites being occupied by the adsorbent upon equilibrium. Therefore, the adsorbent has become exhausted and needs to be replaced. The spent adsorbent is considered solid hazardous waste and is usually dumped into the landfill site or incinerated, which creates environmental problems [67].

Nevertheless, researchers are working on solutions, and one of the outcomes is through a recovery or regeneration process. From the economic and environmental point of view, the recovery process is a vital aspect to focus upon. The disposal of hazardous spent adsorbent creates various environmental implications, and a recovery method can reduce the problem. Various recovery methods have been utilised with differing degrees of success. These methods include regeneration and desorption

processes. Various techniques are available to regenerate the exhausted adsorbent, but the desorption method is the most preferred technique for its economical and effective regeneration process factors. The desorption process includes thermal, electrochemical, ultrasonic, and chemical methods where the solvents are called eluting agents [65]. Spent adsorbent is washed with water and then treated with an eluting agent through batch or column treatment. Then, the treated adsorbent is flushed with water to remove eluting agent from the adsorbent, making it ready for further adsorption.

The feasibility of the desorption process lies on the desorption efficiency and regeneration cycles [35] where, based on the literature, most of the adsorbents can regenerate to an average of 4–5 cycles with 80–85 % removal [63,66]. It can be concluded that regeneration, reuse of adsorbent, and recovery of solute are vital aspects of adsorption that need to be considered when applying them in industrial-scale applications. Subsequently, used SMC biochar can be used for carbonisation in the agricultural industry. The reuse of spent biochar as fertilisers is an effective approach that should be considered in the future. By burying the spent biochar, it can improve crop yields as the metal ions coated biochar contains all the necessary metals as nutrients to enhance crop production [26].

3.7.2. Comparison of adsorption capacities of SMC biochar with previously reported adsorbent

The application of SMC as biochar is still relatively new in the research field, especially its application as filter media in mine-impacted water. Table 10 summarises the adsorption capacities from other previously reported feedstock biochars. Compared to other feedstock biochar, SMC shows great adsorption capacity. The adsorption capacity for Pb, Cu, Mn and Fe was shown to be 16.218 mg/g, 49.833 mg/g, 6.665 mg/g and 33.186 mg/g, respectively, which is higher than pinewood, sewage sludge, rice husk and manure biochars. However, the Pb adsorption for SMC biochar was lower than rice husk biochar but was higher than other types of biochar.

Additionally, the adsorption capacity of SMC biochar in this study was much higher than that of other SMC biochar from the literature. There are many factors contributing to this predicament, including pyrolysis production and the experimental conditions involved. Henceforth, from this study and Table 10, it is concluded that SMC biochar is an ideal adsorbent for removing heavy metals and has the potential to be a filter media in a heavy metal retention system for mining water treatment.

Table 10
Comparison of the adsorption capacities of SMC biochar towards heavy metal removal.

Biochar	Heavy metals	Adsorption capacity (mg/g)	References	
Rice husk	Cu	37.5	([55]; [8])	
	Pb	43.9		
	Zn	34.3		
Corn stalk	Pb	0.3	[3]	
Hickory wood	Pb	22.82	([32]; [57])	
	Cu	15.7		
Peanut shell	Pb	30.29	[45]	
	Cu	18.39		
	Zn	6.67		
Pinewood	Pb	4.91	([58]; [59])	
Spent mushroom compost biochar	Mn	3.341	[60]	
	Pb	61.09		
	Cu	15.81		
	Zn	2.59		
	Pb	17.344		This study
	Cu	49.833		
	Mn	7.665		
Fe	32.186			

4. Conclusion

This study investigates the efficacy and feasibility of biochar derived from spent mushroom compost (SMC) as a sustainable solution for the removal of heavy metals (Cu, Mn, Fe, and Pb) commonly found in abandoned mine water. The findings emphasize the significant role of pyrolysis temperature in optimising the adsorption performance of SMC biochar. Among the tested biochars, SMC biochar pyrolysed at 500 °C (B500) demonstrated an impressive heavy metal removal efficiency of 97.43 %, with an adsorption capacity of 2.398 mg/g. Although B700 showed a slightly higher removal rate of 98.38 %, the comparable performance of B500 highlights its practicality due to lower production energy requirements and costs. Adsorption isotherms and kinetic studies further validated the performance of SMC biochar. The Langmuir isotherm model and pseudo-second-order kinetics exhibited excellent fitting ($R^2 > 0.99$), confirming monolayer adsorption as the dominant mechanism. These findings provide valuable insights into the adsorption processes, reinforcing SMC biochar's capacity to effectively remove heavy metals from contaminated water.

In addition to its adsorption efficiency, this study highlights the economic feasibility of SMC biochar as a filter medium. With a production cost of RM 1000/t, SMC biochar is significantly more cost-effective than conventional activated carbon (RM 10,000/t). Furthermore, the material's high reusability, retaining over 85 % adsorption efficiency after five cycles, enhances its long-term viability in water treatment applications. The study also discusses the potential for metal recovery, enabling the recovery of valuable metals such as Cu and Pb during desorption processes, which can further offset operational costs and contribute to circular economy principles.

In conclusion, this study showcases the premise of SMC biochar, particularly at 500 °C, as a sustainable, cost-effective, and environmentally friendly solution for heavy metal removal in mine-impacted water. Its high adsorption efficiency, scalability, and alignment with Sustainable Development Goal 6 make it a valuable innovation in addressing water contamination and waste management challenges in mining-affected regions. By integrating low production costs, reusability, and metal recovery, SMC biochar offers a holistic solution that bridges environmental and economic sustainability.

CRedit authorship contribution statement

Zafira Madzin: Writing – original draft, Investigation, Formal analysis, Conceptualization. **Izni Zahidi:** Writing – review & editing, Supervision. **Amin Talei:** Writing – review & editing. **Mavinakere Eshwaraiah Raghunandan:** Writing – review & editing. **Andreas Aditya Hermawan:** Methodology. **Daljit Singh Karam:** Writing – review & editing.

Consent to participate

Not applicable.

Consent to publish

Not applicable.

Ethical approval

Not applicable.

Declaration of competing interest

The authors declare that they have no known competing financial interests or personal relationships that could have appeared to influence the work reported in this paper.

Acknowledgement

The authors express their appreciation to Monash University Malaysia for the funding and support throughout this research.

Data availability

Data will be made available on request.

References

- [1] Z. Madzin, F.M. Kusin, F.M. Yusof, S.N. Muhammad, Assessment of water quality index and heavy metal contamination in active and abandoned iron ore mining sites in Pahang, Malaysia. MATEC Web of Conferences 103 (2017), <https://doi.org/10.1051/mateconf/201710305010>.
- [2] F.M. Kusin, N.A. Sulong, F.N.A. Affandi, V.L.M. Molahid, S. Jusop, Prospect of abandoned metal mining sites from a hydrogeochemical perspective, Environ. Sci. Pollut. Res. 28 (3) (2021) 2678–2695, <https://doi.org/10.1007/s11356-020-10626-1>.
- [3] S. Yan, W. Yu, T. Yang, Q. Li, J. Guo, The adsorption of corn stalk biochar for Pb and Cd: preparation, characterization, and batch adsorption study, Separations 9 (2) (2022), <https://doi.org/10.3390/separations9020022>.
- [4] I.I. Ruzi, A.R. Ishak, M.A. Abdullah, N.N.M. Zain, A.R. Tualeka, R. Adriyani, R. Mohamed, H.A. Edinur, M.Y. Aziz, Heavy metal contamination in Sungai Petani, Malaysia: a wastewater-based epidemiology study, J. Water Health 22 (6) (2024) 953–966, <https://doi.org/10.2166/wh.2024.241>.
- [5] M. Zeb, K. Khan, M. Younas, A. Farooqi, X. Cao, Y.N. Kavil, S.S. Alelyani, M. M. Alkasbi, A.G. Al-Sehemi, A review of heavy metals pollution in riverine sediment from various Asian and European countries: Distribution, sources, and environmental risk. In *Marine Pollution Bulletin*. 2024. Elsevier Ltd, 2024, <https://doi.org/10.1016/j.marpolbul.2024.116775>.
- [6] L.S. Mazilamani, K.V. Annammala, P. Martin, L.Y. Qi, D. Sugumaran, Y.E. Ling, P. S. Reynard, A. Nurhidayat, M.S. Syawal, I.D.A. Sutapa, Comprehensive Assessment of Water and Sediment Quality to Support Sustainable Management Practices and Mitigate Potential Risks of Trace Metal Pollution in the Johor River Basin, Ecotoxicology and Hydrobiology, South Peninsular Malaysia, 2024, <https://doi.org/10.1016/j.ecohyd.2024.04.009>.
- [7] N.A. Shukor, K. Krishnan, W.L. Shing, N. Ariffin, W.L. Yong, The pollution characteristics of harmful heavy metal in surface sediment of Sepang River, Malaysia. Environ. Ecol. Res. 11 (4) (2023) 579–585, <https://doi.org/10.13189/eer.2023.110406>.
- [8] N.S.M. Razali, M. Ikhwanuddin, M. Maulidiani, N.J. Gooderham, M. Alam, N.H. A. Kadir, Ecotoxicological impact of heavy metals on wild mud crabs (*Scylla olivacea*) in Malaysia: an integrative approach of omics, molecular docking and human risk assessment, Sci. Total Environ. 946 (2024), <https://doi.org/10.1016/j.scitotenv.2024.174210>.
- [9] B.K. Biswal, K. Vijayaraghavan, D.L. Tsen-Tieng, R. Balasubramanian, Biochar-based bioretention systems for removal of chemical and microbial pollutants from stormwater: A critical review. In *Journal of Hazardous Materials* (Vol. 422). Elsevier B.V., 2022, <https://doi.org/10.1016/j.jhazmat.2021.126886>.
- [10] S. Wu, F. Xie, S. Chen, B. Fu, The removal of Pb (II) and Cd (II) with hydrous manganese dioxide: mechanism on zeta potential and adsorption behavior, Environ. Technol. (United Kingdom) 41 (24) (2020) 3219–3232, <https://doi.org/10.1080/09593330.2019.1604814>.
- [11] R. A. L. Srinivasan, N. Arumugam, A. Abdulrahman I., M. Sakkarapalayam M., V. A. Biosorption efficacy studies of *Sargassum wightii* and its biochar on the removal of chromium from aqueous solution, J. Taiwan Inst. Chem. Eng. (2023), <https://doi.org/10.1016/j.jtice.2023.105241>.
- [12] K.H. Hama Aziz, R. Kareem, Recent advances in water remediation from toxic heavy metals using biochar as a green and efficient adsorbent: A review, Case Stud. Chem. Environ. Eng. 8 (2023), <https://doi.org/10.1016/j.csee.2023.100495>.
- [13] Z. Li, M. Li, T. Zheng, Y. Li, X. Liu, Chemosphere removal of tylosin and copper from aqueous solution by biochar stabilized nano-hydroxyapatite, Chemosphere 235 (2019) 136–142, <https://doi.org/10.1016/j.chemosphere.2019.06.091>.
- [14] Z. Li, X. Meng, Z. Zhang, Equilibrium and kinetic modelling of adsorption of rhodamine B on MoS₂, Mater. Res. Bull. 111 (November 2018) (2019) 238–244, <https://doi.org/10.1016/j.materresbull.2018.11.012>.
- [15] X. Chen, S. Jiang, J. Wu, X. Yi, G. Dai, Y. Shu, Three-year field experiments revealed the immobilization effect of natural aging biochar on typical heavy metals (Pb, Cu, Cd), Sci. Total Environ. 912 (2024), <https://doi.org/10.1016/j.scitotenv.2023.169384>.
- [16] I.B. Koki, K.H. Low, H. Juahir, M. Abdul Zali, A. Aziz, S.M. Zain, Consumption of water from ex-mining ponds in Klang Valley and Melaka, Malaysia: A health risk study, Chemosphere 195 (2018) 641–652, <https://doi.org/10.1016/j.chemosphere.2017.12.112>.
- [17] V. Singh, N. Pant, R.K. Sharma, D. Padalia, P.S. Rawat, R. Goswami, P. Singh, A. Kumar, P. Bhandari, A. Tabish, A.M. Deifalla, Adsorption studies of Pb(II) and Cd (II) heavy metal ions from aqueous solutions using a magnetic biochar composite material, Separations 10 (7) (2023), <https://doi.org/10.3390/separations10070389>.
- [18] Q.M. Truong, T.B. Nguyen, W.H. Chen, C.W. Chen, A.K. Patel, X.T. Bui, R. R. Singhanian, C.Di. Dong, Removal of heavy metals from aqueous solutions by high performance capacitive deionization process using biochar derived from

- Sargassum hemiphyllum, *Bioresour. Technol.* 370 (2023), <https://doi.org/10.1016/j.biortech.2022.128524>.
- [19] M.M. Abdallah, M.N. Ahmad, G. Walker, J.J. Leahy, W. Kwapinski, Batch and Continuous Systems for Zn, Cu, and Pb Metal Ions Adsorption on Spent Mushroom Compost Biochar [Research-article], *Ind. Eng. Chem. Res.* 58 (2019) 7296–7307, <https://doi.org/10.1021/acs.iecr.9b00749>.
- [20] Y. Jin, M. Zhang, Z. Jin, G. Wang, R. Li, X. Zhang, X. Liu, J. Qu, H. Wang, Characterization of biochars derived from various spent mushroom substrates and evaluation of their adsorption performance of Cu(II) ions from aqueous solution, *Environ. Res.* February. (2020), <https://doi.org/10.1016/j.envres.2020.110323>.
- [21] Z. Shen, J. Zhang, D. Hou, D.C.W. Tsang, Y.S. Ok, D.S. Alessi, Synthesis of MgO-coated corn cob biochar and its application in lead stabilization in a soil washing residue, *Environ. Int.* 122 (September 2018) 357–362, <https://doi.org/10.1016/j.envint.2018.11.045>.
- [22] M. Burachevskaya, T. Minkina, T. Bauer, I. Lobzenko, A. Fedorenko, M. Mazarji, S. Shukhova, S. Mandzhieva, A. Nazarenko, V. Butova, M.H. Wong, V.D. Rajput, Fabrication of biochar derived from different types of feedstocks as an efficient adsorbent for soil heavy metal removal, *Sci. Rep.* 13 (1) (2023), <https://doi.org/10.1038/s41598-023-27638-9>.
- [23] F.A. Dawodu, K.G. Akpomie, Simultaneous adsorption of Ni(II) and Mn(II) ions from aqueous solution onto a Nigerian kaolinite clay, *J. Mater. Res. Technol.* 3 (2) (2014) 129–141, <https://doi.org/10.1016/j.jmrt.2014.03.002>.
- [24] B. Qiu, X. Tao, H. Wang, W. Li, X. Ding, H. Chu, Biochar as a low-cost adsorbent for aqueous heavy metal removal: A review. In *Journal of Analytical and Applied Pyrolysis* (Vol. 155). Elsevier B.V, 2021, <https://doi.org/10.1016/j.jaap.2021.105081>.
- [25] V. Manirethan, N. Gupta, R.M. Balakrishnan, K. Raval, Batch and continuous studies on the removal of heavy metals from aqueous solution using biosynthesized melanin-coated PVDF membranes. *ii*, 2019.
- [26] H. Patel, Comparison of batch and fixed bed column adsorption: a critical review, *Int. J. Environ. Sci. Technol.* 19 (10) (2022) 10409–10426, <https://doi.org/10.1007/s13762-021-03492-y>.
- [27] A.S. Eltaweil, H. Ali Mohamed, E.M. Abd El-Monaem, G.M. El-Subruiti, Mesoporous magnetic biochar composite for enhanced adsorption of malachite green dye: characterization, adsorption kinetics, thermodynamics and isotherms, *Adv. Powder Technol.* 31 (3) (2020) 1253–1263, <https://doi.org/10.1016/j.apt.2020.01.005>.
- [28] S. Chen, C. Qin, T. Wang, F. Chen, X. Li, H. Hou, M. Zhou, Study on the adsorption of dyestuffs with different properties by sludge-rice husk biochar: adsorption capacity, isotherm, kinetic, thermodynamics and mechanism, *J. Mol. Liq.* 285 (2019) 62–74, <https://doi.org/10.1016/j.molliq.2019.04.035>.
- [29] U. Tyagi, Enhanced adsorption of metal ions onto Vetiveria zizanioides biochar via batch and fixed bed studies, *Bioresour. Technol.* 345 (2022) 126475, <https://doi.org/10.1016/j.biortech.2021.126475>.
- [30] A. Daghbandan, B.A. Souraki, M.A. Zadeh, A comprehensive study on the applicability of tea leaves and rice straw as novel sorbents for iron and manganese removal from running water in a fixed-bed column, *Korean J. Chem. Eng.* 39 (3) (2022) 628–637, <https://doi.org/10.1007/s11814-021-0910-5>.
- [31] K.H.H. Aziz, Removal of toxic heavy metals from aquatic systems using low-cost and sustainable biochar: A review, in: *Desalination and Water Treatment* vol. 320, Elsevier B.V, 2024, <https://doi.org/10.1016/j.dwt.2024.100757>.
- [32] L. Natrayan, S. Kaliappan, C.N. Dheeraj Kumar Reddy, M. Karthick, N. S. Sivakumar, P.P. Patil, S. Sekar, S. Thanappan, Development and characterization of carbon-based adsorbents derived from agricultural wastes and their effectiveness in adsorption of heavy metals in waste water, *Bioinorg. Chem. Appl.* 2022 (2022), <https://doi.org/10.1155/2022/1659855>.
- [33] H. Chaudhary, J. Dinakaran, K.S. Rao, Comparative analysis of biochar production methods and their impacts on biochar physico-chemical properties and adsorption of heavy metals. *Journal of Environmental, Chem. Eng.* 12 (3) (2024), <https://doi.org/10.1016/j.jece.2024.113003>.
- [34] L. Joseph, B.M. Jun, J.R.V. Flora, C.M. Park, Y. Yoon, Removal of heavy metals from water sources in the developing world using low-cost materials: A review, *Chemosphere* 229 (2019) 142–159, <https://doi.org/10.1016/j.chemosphere.2019.04.198>.
- [35] M. Banerjee, N. Bar, S.K. Das, Cu(II) removal from aqueous solution using the walnut Shell: adsorption study, regeneration study, plant scale-up design, economic feasibility, statistical, and GA-ANN modeling, *Int. J. Environ. Res.* 15 (5) (2021) 875–891, <https://doi.org/10.1007/s41742-021-00362-w>.
- [36] Y. Zhao, Y. Li, D. Fan, J. Song, F. Yang, Application of kernel extreme learning machine and kriging model in prediction of heavy metals removal by biochar, *Bioresour. Technol.* 329 (2021), <https://doi.org/10.1016/j.biortech.2021.124876>.
- [37] Y. Jin, C. Teng, S. Yu, T. Song, L. Dong, J. Liang, X. Bai, X. Liu, X. Hu, J. Qu, Batch and fixed-bed biosorption of Cd(II) from aqueous solution using immobilized *Pleurotus ostreatus* spent substrate, *Chemosphere* 191 (2018) 799–808, <https://doi.org/10.1016/j.chemosphere.2017.08.154>.
- [38] R. Zhou, M. Zhang, S. Shao, Optimization of target biochar for the adsorption of target heavy metal ion, *Sci. Rep.* 12 (1) (2022), <https://doi.org/10.1038/s41598-022-17901-w>.
- [39] X. Yang, Y. Wan, Y. Zheng, F. He, Z. Yu, J. Huang, H. Wang, Y.S. Ok, Y. Jiang, B. Gao, Surface functional groups of carbon-based adsorbents and their roles in the removal of heavy metals from aqueous solutions: A critical review, *Chem. Eng. J.* 366 (February) (2019) 608–621, <https://doi.org/10.1016/j.cej.2019.02.119>.
- [40] N. Cheng, B. Wang, P. Wu, X. Lee, Y. Xing, M. Chen, B. Gao, Adsorption of emerging contaminants from water and wastewater by modified biochar: A review, *Environ. Pollut.* 273 (2021), <https://doi.org/10.1016/j.envpol.2021.116448>.
- [41] J.O. Ighalo, A.G. Adeniyi, O.A.A. Eletta, L.T. Arowoyele, Competitive adsorption of Pb(II), Cu(II), Fe(II) and Zn(II) from aqueous media using biochar from oil palm (*Elaeis guineensis*) fibers: a kinetic and equilibrium study, *Indian Chem. Eng. II* 1–11 (2020), <https://doi.org/10.1080/00194506.2020.1787870>.
- [42] N. Esfandiari, R. Suri, E.R. McKenzie, Competitive sorption of Cd, Cr, Cu, Ni, Pb and Zn from stormwater runoff by five low-cost sorbents; effects of co-contaminants, humic acid, salinity and pH, *J. Hazard. Mater.* 423 (2022), <https://doi.org/10.1016/j.jhazmat.2021.126938>.
- [43] H.L. Chen, T.K. Nath, S. Chong, V. Foo, C. Gibbins, A.M. Lechner, The plastic waste problem in Malaysia: management, recycling and disposal of local and global plastic waste. *SN, Appl. Sci.* 3 (4) (2021), <https://doi.org/10.1007/s42452-021-04234-y>.
- [44] S. Sahu, S. Pahi, S. Tripathy, S.K. Singh, A. Behera, U.K. Sahu, R.K. Patel, Adsorption of methylene blue on chemically modified lychee seed biochar: dynamic, equilibrium, and thermodynamic study, *J. Mol. Liq.* 315 (2020), <https://doi.org/10.1016/j.molliq.2020.113743>.
- [45] R. Shan, Y. Shi, J. Gu, Y. Wang, H. Yuan, Single and competitive adsorption affinity of heavy metals toward peanut shell-derived biochar and its mechanisms in aqueous systems, *Chin. J. Chem. Eng.* 28 (5) (2020) 1375–1383, <https://doi.org/10.1016/j.cjche.2020.02.012>.
- [46] B.J. Ni, Q.S. Huang, C. Wang, T.Y. Ni, J. Sun, W. Wei, Competitive adsorption of heavy metals in aqueous solution onto biochar derived from anaerobically digested sludge. In *Chemosphere* (Vol. 219, pp. 351–357), 2019, <https://doi.org/10.1016/j.chemosphere.2018.12.053>.
- [47] H. Huang, N.G. Reddy, X. Huang, P. Chen, P. Wang, Y. Zhang, Y. Huang, P. Lin, A. Garg, Effects of pyrolysis temperature, feedstock type and compaction on water retention of biochar amended soil, *Sci. Rep.* 11 (1) (2021) 1–19, <https://doi.org/10.1038/s41598-021-86701-5>.
- [48] Z. Mahdi, A. El Hanandeh, Q.J. Yu, Journal of Environmental Chemical Engineering Preparation, characterization and application of surface modified biochar from date seed for improved lead, copper, and nickel removal from aqueous solutions, *J. Environ. Chem. Eng.* 7 (5) (2019) 103379, <https://doi.org/10.1016/j.jece.2019.103379>.
- [49] D. Mohan, V. Choudhary, M. Patel, C.U. Pittman, Batch and continuous fixed-bed lead removal using Himalayan pine needle biochar: isotherm and kinetic studies, *ACS Omega* 5 (27) (2020) 16366–16378, <https://doi.org/10.1021/acsomega.0c00216>.
- [50] L. Verma, J. Singh, Removal of As(III) and As(V) from aqueous solution using engineered biochar: batch and fixed-bed column study, *Int. J. Environ. Sci. Technol.* 1961–1980 (2022), <https://doi.org/10.1007/s13762-022-03920-7>.
- [51] B.L. Liu, M.M. Fu, L. Xiang, N.X. Feng, H.M. Zhao, Y.W. Li, Q.Y. Cai, H. Li, C.H. Mo, M.H. Wong, Adsorption of microcystin contaminants by biochars derived from contrasting pyrolytic conditions: characteristics, affecting factors, and mechanisms, *Sci. Total Environ.* 763 (2021), <https://doi.org/10.1016/j.scitotenv.2020.143028>.
- [52] A. Jayakumar, C. Wurzer, S. Soldatou, C. Edwards, L.A. Lawton, O. Mašek, New directions and challenges in engineering biologically-enhanced biochar for biological water treatment, *Sci. Total Environ.* 796 (2021), <https://doi.org/10.1016/j.scitotenv.2021.148977>.
- [53] W. Liao, X. Zhang, S. Ke, J. Shao, H. Yang, S. Zhang, H. Chen, The influence of biomass species and pyrolysis temperature on carbon-retention ability and heavy metal adsorption property during biochar aging, *Fuel Process. Technol.* 240 (2023), <https://doi.org/10.1016/j.fuproc.2022.107580>.
- [54] M.T.H. Siddiqui, S. Nizamuddin, N.M. Mubarak, K. Shirin, M. Aijaz, M. Hussain, H. A. Baloch, Characterization and process optimization of biochar produced using novel biomass, waste pomegranate Peel: A response surface methodology approach, *Waste Biomass Valoriz.* 10 (3) (2019) 521–532, <https://doi.org/10.1007/s12649-017-0091-y>.
- [55] L. Campion, M. Bekchanova, R. Malina, T. Kuppens, The costs and benefits of biochar production and use: A systematic review, in: *Journal of Cleaner Production* vol. 408, Elsevier Ltd., 2023, <https://doi.org/10.1016/j.jclepro.2023.137138>.
- [56] R.W. Mwangi, M. Mustafa, N. Kappel, L. Csabalki, A. Szabó, Practical applications of spent mushroom compost in cultivation and disease control of selected vegetables species. In *Journal of Material Cycles and Waste Management* (Vol. 26, Issue 4, pp. 1918–1933). Springer, 2024, <https://doi.org/10.1007/s10163-024-01969-9>.
- [57] S. Wei, M. Zhu, X. Fan, J. Song, P. Peng, K. Li, W. Jia, H. Song, Influence of pyrolysis temperature and feedstock on carbon fractions of biochar produced from pyrolysis of rice straw, pine wood, pig manure and sewage sludge, *Chemosphere* 218 (2019) 624–631, <https://doi.org/10.1016/j.chemosphere.2018.11.177>.
- [58] T. Bandara, J. Xu, I.D. Potter, A. Franks, J.B.A.J. Chathurika, C. Tang, Mechanisms for the removal of Cd(II) and Cu(II) from aqueous solution and mine water by biochars derived from agricultural wastes, *Chemosphere* 254 (2020), <https://doi.org/10.1016/j.chemosphere.2020.126745>.
- [59] M. Imran-Shaukat, R. Wahi, Z. Ngaini, The application of agricultural wastes for heavy metals adsorption: A meta-analysis of recent studies, *Biores. Technol. Rep.* 17 (2022), <https://doi.org/10.1016/j.biteb.2021.100902>.
- [60] K. Yunus, M.A. Zuraidah, A. John, A review on the accumulation of heavy metals in coastal sediment of peninsular Malaysia, *Ecofem. Climate Change* 1 (1) (2020) 21–35, <https://doi.org/10.1108/ecfc-03-2020-0003>.
- [61] Z. Madzin, I. Zahidi, M.E. Raghunandan, A. Talei, Potential application of spent mushroom compost (SMC) biochar as low-cost filtration media in heavy metal removal from abandoned mining water: a review, 2022, 1023456789.
- [62] G.N. Paravavithana, K. Kawamoto, Y. Inoue, T. Saito, Adsorption of Cd²⁺ and Pb²⁺ onto coconut shell biochar and biochar-mixed soil, *Environ. Earth Sci.* 75 (6) (2016) 1–12, <https://doi.org/10.1007/s12665-015-5167-z>.

- [63] M. Banerjee, R.K. Basu, S.K. Das, Cr(VI) adsorption by a green adsorbent walnut shell: Adsorption studies, regeneration studies, scale-up design and economic feasibility, *Proc. Safe. Environ. Protect.* 116 (2018) 693–702, <https://doi.org/10.1016/j.psep.2018.03.037>.
- [64] Y. Dai, N. Zhang, C. Xing, Q. Cui, Q. Sun, The adsorption, regeneration and engineering applications of biochar for removal organic pollutants: A review, *Chemosphere* 223 (2019) 12–27, <https://doi.org/10.1016/j.chemosphere.2019.01.161>.
- [65] S. Kulkarni, J. Kaware, *Regeneration and Recovery in Adsorption- a Review*, *Intern. J. Innov. Sci. Eng. Technol. (IJSET)* 1 (8) (2014) 61–64.
- [66] S. Lata, P.K. Singh, S.R. Samadder, Regeneration of adsorbents and recovery of heavy metals: a review, *Intern. J. Environ. Sci. Technol.* 12 (4) (2015) 1461–1478, <https://doi.org/10.1007/s13762-014-0714-9>.
- [67] M. Vakili, S. Deng, G. Cagnetta, W. Wang, P. Meng, Separation and Purification Technology Regeneration of chitosan-based adsorbents used in heavy metal adsorption : A review, *Separ. Purif. Technol.* 224 (2019 February) 373–387, <https://doi.org/10.1016/j.seppur.2019.05.040>.
- [68] J. Wang, S. Wang, Preparation, modification and environmental application of biochar: A review, *J. Clean. Prod.* 227 (2019) 1002–1022, <https://doi.org/10.1016/j.jclepro.2019.04.282>.
- [69] X. Zheng, H. Nguyen, A novel artificial intelligent model for predicting water treatment efficiency of various biochar systems based on artificial neural network and queuing search algorithm, *Chemosphere* 287 (2022), <https://doi.org/10.1016/j.chemosphere.2021.132251>.
- [70] Healy, J. Ministry of Health, Malaysia Nour Hanah Othman, Ministry of Health, Malaysia Kalsom Maskon, Ministry of Health, Malaysia Abdul Rahim Abdullah, Ministry of Health (Vol. 3, Issue 1). (2013), doi:Ministry.